UNIVERSITÄTSKLINIKUM HAMBURG - EPPENDORF

Klinik und Poliklinik für Herz- und Gefäßchirurgie

Direktor Prof. Dr. Dr. Hermann Reichenspurner

Comparison of microstructural alterations in the proximal aorta between aortic stenosis and regurgitation

Dissertation

zur Erlangung des Grades eines Doktors der Medizin

an der Medizinischen Fakultät der Universität Hamburg.

vorgelegt von:

Tatiana Maria Sequeira Gross

aus Nicaragua

Hamburg 2020

Angenommen von der
Medizinischen Fakultät der Universität Hamburg am: 29.04.2021

Veröffentlicht mit Genehmigung der
Medizinischen Fakultät der Universität Hamburg.

Prüfungsausschuss, der Vorsitzende: Prof. Dr. Yskert von Kodolitsch

Prüfungsausschuss, zweiter Gutachter: Prof. Dr. Evaldas Girdauskas

Table of Contents

Comparison of microstructural alterations in the proximal aorta between aortic stenosis and regurgitation

Tatiana M. Sequeira Gross, MD,[a] Diana Lindner, PhD,[b,c] Francisco M. Ojeda, PhD,[b] Johannes Neumann, MD,[b,c] Nimrat Grewal, MD,[d] Thomas Kuntze, MD,[e] Stefan Blankenberg, MD,[b,c] Hermann Reichenspurner, MD, PhD,[a,c] Dirk Westermann, MD,[b,c] and Evaldas Girdauskas, MD[a,c]

ABSTRACT

Objective: We aimed to analyze the association among flow patterns, gene expression, and histologic alterations of the proximal aorta in patients with aortic valve disease.

Methods: A total of 131 patients referred for aortic valve replacement were grouped by valve dysfunction (aortic stenosis vs aortic regurgitation) and valve morphology (bicuspid vs tricuspid). On the basis of magnetic resonance imaging, aortic tissue from outer and inner curvature was collected for gene expression and histologic analysis. To identify differences in aortic remodeling, age- and sex-adjusted data for inflammation (*CCL2*, *VCAM1*, inflammation and atherosclerosis) and medial degeneration (*COL1A1*, *ELN*, fibrosis, elastin fragmentation, and cystic medial necrosis) were compared.

Results: First, we compared all patients with aortic regurgitation (n = 64) and patients with aortic stenosis (n = 67). In patients with aortic regurgitation, *COL1A1* expression and all histologic markers were significantly increased. With respect to aortic diameter, all subsequent analyses were refined by considering only individuals with aortic diameter 40 mm or greater. Second, patients with bicuspid aortic valve were compared, resulting in a similar aortic diameter. Although patients with aortic regurgitation were younger, no differences were found in gene expression or histologic level. Third, valve morphology was compared in patients with aortic regurgitation. Although aortic diameter was similar, patients with regurgitant bicuspid aortic valve were younger than patients with regurgitant tricuspid aortic valve. Inflammatory markers were similar, whereas markers for medial degeneration were increased in patients with regurgitant tricuspid aortic valve.

Conclusions: Our results indicate that the proximal aorta in patients with aortic regurgitation showed an increased inflammation and medial degeneration compared with patients with aortic stenosis. Refining both groups by valve morphology, in patients with bicuspid aortic valve, no difference except age was detected between aortic regurgitation and aortic stenosis. In patients with aortic regurgitation, tricuspid aortic valve revealed increased markers for medial degeneration but no differences regarding inflammatory markers. (J Thorac Cardiovasc Surg 2020;■:1-12)

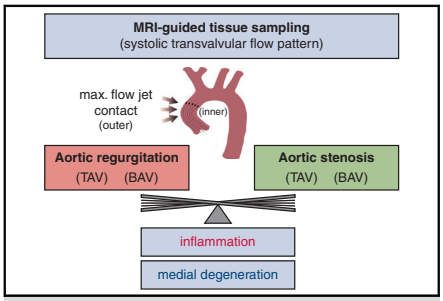

Aortic inflammation and medial degeneration differ between regurgitation and stenosis.

CENTRAL MESSAGE

Compared with stenosis, aortic tissue from patients with regurgitation revealed increased inflammation and even more medial degeneration, which was aggravated in patients with tricuspid valve morphology.

PERSPECTIVE

Compared with patients with stenosis, aortic tissue derived from patients with regurgitation presented more severe vascular remodeling, which was even more pronounced in those patients with tricuspid valve morphology. Severe vascular remodeling may result in faster aortic dilation; therefore, regurgitation should be considered as a possible risk factor to prevent future complications.

See Commentary on page XXX.

MIS

From the [a]Clinic for Cardiovascular Surgery, and [b]Clinic for Cardiology, University Heart and Vascular Center Hamburg, Hamburg, Germany; [c]DZHK (German Center for Cardiovascular Research), Partner Site Hamburg/Kiel/Lübeck, Hamburg, Germany; [d]Clinic of Cardiovascular Surgery, Leiden University Medical Center, Leiden, Netherlands; and [e]Clinic of Cardiac Surgery, Central Hospital Bad Berka, Bad Berka, Germany.

This study was supported by the UHZ Stiftung Herz im Zentrum and the German Center of Cardiovascular Research (DZHK).

Drs Sequeira Gross, Lindner, Westermann, and Girdauskas contributed equally.

Received for publication Sept 2, 2019; revisions received Feb 24, 2020; accepted for publication March 3, 2020.

Address for reprints: Evaldas Girdauskas, MD, Department of Cardiovascular Surgery, University Heart and Vascular Center Hamburg, Martinistraße 52, 20246 Hamburg, Germany (E-mail: e.girdauskas@uke.de).

0022-5223/$36.00

https://doi.org/10.1016/j.jtcvs.2020.03.002

Abbreviations and Acronyms

AD = aortic diameter
AR = aortic regurgitation
AS = aortic stenosis
BAV = bicuspid aortic valve
CMN = cystic medial necrosis
MRI = magnetic resonance imaging
TAV = tricuspid aortic valve
WSS = wall shear stress

Scanning this QR code will take you to the article title page to access supplementary information.

MIS

Ascending aortic dilation is the most common aortic pathological condition associated with an elevated risk of dissection or rupture.[1] Because of its silent nature, there exists an urgent need of better understanding of risk factors and pathophysiology. Previous studies suggested that structural alterations of the aortic wall are mainly caused by a variable interaction between genetic predisposition and altered hemodynamics.[2-5]

Genetic predisposition is usually associated with congenital aortic wall weakness, such as in Loeys–Dietz and Marfan syndrome.[6] However, the hemodynamics in the proximal aorta may exhibit variable flow patterns and is influenced by functional aortic root elements, the aortic valve being one of the most important. A normal tricuspid aortic valve (TAV) induces steady laminar flow pattern in the proximal aorta, as demonstrated by 4-dimensional flow magnetic resonance imaging (MRI) analysis.[7] In contrast, patients with an aortic valve dysfunction (aortic stenosis [AS] or aortic regurgitation [AR]) exhibit different flow and wall shear stress (WSS) patterns in the proximal aorta.[7]

Recent data indicate that elevated WSS due to aortic valve dysfunction can alter gene expression in the aortic wall and further induce microstructural lesions, which finally lead to changes in vessel geometry. This process is also known as ''aortic remodeling.''[8,9] In the present study, we aim to analyze the association among transvalvular flow patterns, gene expression, and histologic alterations of the proximal aorta in patients with aortic valve disease. Because of the marked heterogeneity of the study population, age- and sex-adjusted comparisons were made on the basis of valve dysfunction and morphology.

MATERIAL AND METHODS

Study Population

We prospectively identified 131 consecutive patients who were referred for aortic valve surgery with or without proximal aortic surgery from 2012 to 2016. All patients who underwent urgent surgical procedures (eg, acute aortic dissection or endocarditis) were excluded from this study. We excluded all patients who were diagnosed with congenital connective tissue disorders. The diagnosis of valve dysfunction and morphology was based on echocardiographic and cardiac MRI.

Our study design is presented in Figure 1. On the basis of valve dysfunction (AR and AS) and valve morphology (BAV and TAV), several comparisons adjusted for age and sex were analyzed. First, in comparison 1a, all patients with AR (n = 64) were compared with all patients with AS (n = 67). Likewise, in comparison 1b, patients with AR (n = 58) were compared with patients with AS (n = 44) refined by aortic diameter (AD) 40 mm or greater. Comparison 2 used patients with AR and patients with AS refined by bicuspid aortic valve (BAV) morphology and AD 40 mm or greater (AR-BAV, n = 18 and AS-BAV, n = 40). In comparison 3, patients with AR with BAV (AR-BAV, n = 18) were compared with patients with AR with TAV (AR-TAV, n = 40) (Video 1).

The present study conformed to the principles outlined in the Declaration of Helsinki. All patients provided their written informed consent, and the protocol was approved by the Thuringian Chamber of Physicians Ethics Committee (23333/2014/146).

Aortic Tissue Samples Based on Magnetic Resonance Imaging

All patients underwent a noncontrast cardiac MRI (Avanto 1.5T scanner; Siemens, Erlangen, Germany), including phase-velocity encoded imaging of the left ventricular outflow tract and the proximal aorta. Proximal AD was determined as the largest cross-section observed perpendicular to the aortic axis curve in a mid-vessel slice. Structural breath-held, steady-state free precession images were acquired to visually identify the turbulent flow jet in stenotic or regurgitant aortic valves. Using steady-state free precession images, we determined the area of proximal aorta exposed to maximal flow-jet, mostly the outer curvature, as well as the contralateral ''low-flow'' area, mostly the inner curvature. In patients without a jet, aortic samples were obtained from standard aortotomy height before closure. A specific description of samples collection is presented in the Online Data Supplement (Figure E1).

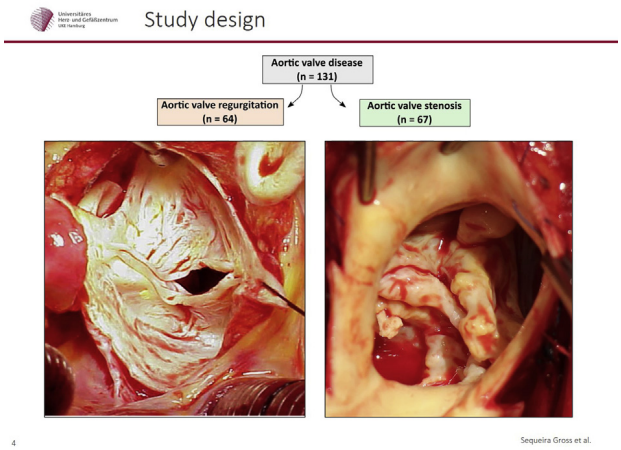

VIDEO 1. Summary of the presented study: Aortic inflammation and medial degeneration differ between regurgitation and stenosis. Video available at: https://www.jtcvs.org/article/S0022-5223(20)30548-1/fulltext.

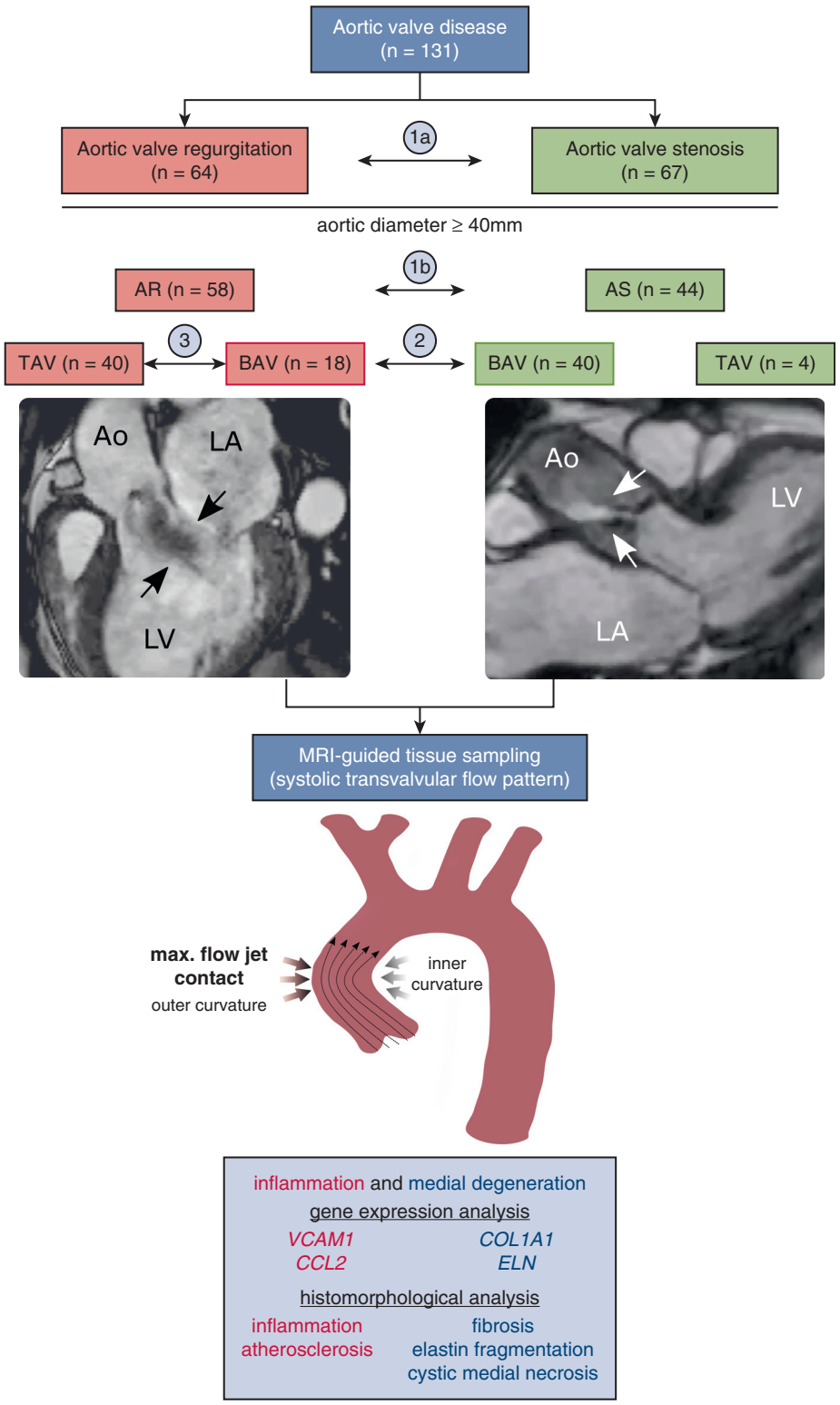

FIGURE 1. Scheme of the study design. A total of 131 patients diagnosed with aortic valve diseases were included in this study. According to valve dysfunction and morphology, 4 comparisons between subgroups were performed. Representative steady-state free precession images demonstrate AR (backflow highlighted with black arrows) or AS (eccentric jet highlighted with white arrows). With the use of MRI, maximal jet impact area was determined in the proximal aorta to guide the collection of aortic samples. Intraoperatively, 1 sample was obtained from the aortic area exposed to jet and another from the contralateral aortic wall. Both samples were investigated regarding markers for inflammation and medial degeneration using gene expression and histomorphologic analysis. *AR,* Aortic regurgitation; *TAV,* tricuspid aortic valve; *BAV,* bicuspid aortic valve; *Ao,* aorta; *LA,* left atrium; *LV,* left ventricle; *MRI,* magnetic resonance imaging.

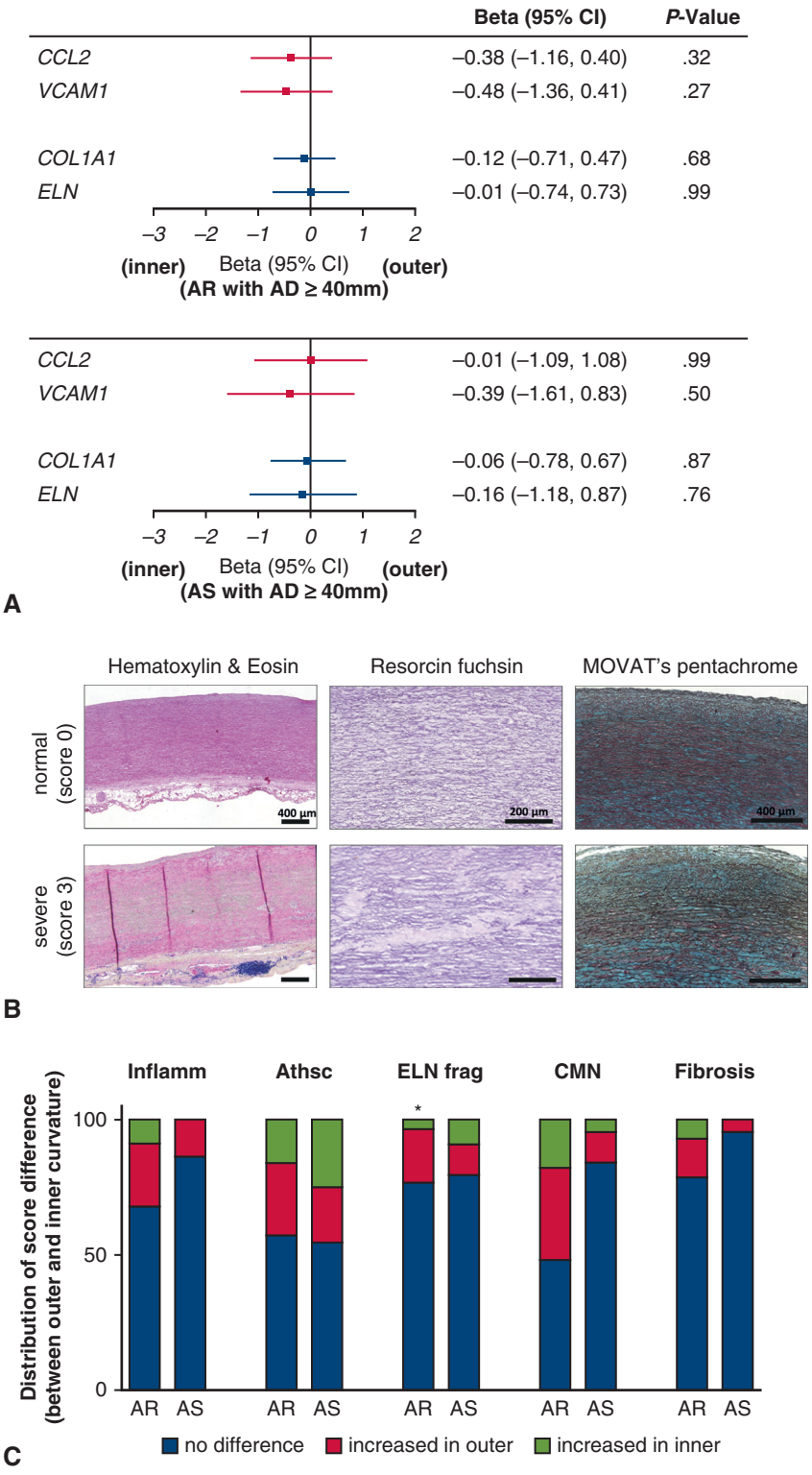

FIGURE 2. Paired differences between outer and inner curvature. A, Gene expression of patients with AD 40 mm or greater were compared between outer and inner curvatures (upper graph: AR, n = 58) (lower graph: AS, n = 44). No differences in the gene expression of *CCL2*, *VCAM1*, *COL1A1,* and *ELN* were detected. Paired comparison of log-transformed gene expression data between outer and inner curvatures was performed using a linear mixed model adjusted for age and sex. The regression coefficient beta is plotted as forest plots for genes associated with inflammation (red) or medial degeneration (blue). B, Representative histologic images of hematoxylin–eosin-stained, resorcin fuchsin–stained, and MOVAT's pentachrome–stained aortic samples. C, Histologic scores of patients with AD 40 mm or greater were compared between outer and inner curvature for patients with AR and AS (comparison 1b). The 5

TABLE 1. Baseline characteristics of study cohort

Comparison 1a	Aortic valve regurgitation (n = 64)	Aortic valve stenosis (n = 67)	*P* value AR vs AS
Male gender, n (%)	46 (71.9)	45 (67.2)	.58
BMI (kg/m^2)	27.1 (23.7-31.2)	28.3 (25.5-32.6)	.28
Comorbidities			
Hyperlipidemia, n (%)	6 (9.4)	3 (4.5)	.69
History of smoking, n (%)	14 (21.9)	16 (23.9)	.81
Diabetes, n (%)	5 (7.8)	11 (16.4)	.92
Arterial hypertension, n (%)	40 (62.5)	45 (67.2)	.47
Bicuspid valve, n (%)	21 (32.8)	59 (88.1)	<.001
Age (y)	59.0 (49.8-66.0)	61.0 (55.5-68.0)	.058
Proximal AD (mm)	52.0 (47.0-58.0)	43.0 (38.5-49.5)	<.001
Comparison 1b (AD ≥40 mm)	**AR ≥ 40 mm (n = 58)**	**AS ≥40 mm (n = 44)**	***P* value AR vs AS**
Male gender, n (%)	40 (69.0)	34 (77.3)	.38
Age (y)	59.0 (49.5-66.0)	62.5 (55.8-69.0)	.041
Proximal AD (mm)	52.5 (49.0-58.8)	47.5 (43.0-52.2)	<.001
Comparison 2 (AD ≥40 mm)	**AR-BAV (n = 18)**	**AS-BAV (n = 40)**	***P* value AR-BAV vs AS-BAV**
Male gender, n (%)	12 (66.7)	32 (80.0)	.33
Age (y)	51.0 (47.2-57.0)	63.0 (55.8-69.0)	<.001
Proximal AD (mm)	51.0 (49.0-55.0)	48.5 (43.8-53.0)	.052
Comparison 3 (AD ≥40 mm)	**AR-BAV (n = 18)**	**AR-TAV (n = 40)**	***P* value AR-BAV vs AR-TAV**
Male gender, n (%)	12 (66.7)	28 (70.0)	1.00
Age (y)	51.0 (47.2-57.0)	61.0 (54.8-69.0)	.002
Proximal AD (mm)	51.0 (49.0-55.0)	53.0 (49.0-60.0)	.46

Continuous variables are given as median (25th percentile, 75th percentile). Binary variables are given as absolute number (relative frequency). *P* values are calculated using Mann–Whitney test for continuous variables and Fisher exact test for binary variables. *AR,* Aortic regurgitation; *AS,* aortic stenosis; *BMI,* body mass index; *AD,* aortic diameter; *BAV,* bicuspid aortic valve; *TAV,* tricuspid aortic valve.

Both collected tissue samples were divided to perform gene expression analysis and histologic staining. Samples for histopathologic analysis were fixed in neutral-buffered formalin, and samples for gene expression analysis were snap-frozen in liquid nitrogen. As indicated in Figure 1, subsequent analysis was designed to address inflammatory markers such as the endothelial adhesion molecule *VCAM1*, the chemo-attractive chemokine *CCL2* on gene expression level, and the infiltrated inflammatory cells and atherosclerosis on histologic tissue sections. Furthermore, we focused on markers for medial degeneration. Therefore, we measured gene expression of the extracellular matrix proteins *COL1A1* and *ELN* and fibrosis, elastin fragmentation, and cystic medial necrosis (CMN) on histologic tissue sections.

Histopathologic Analysis

The 5 histologic parameters were semiquantitatively graded according to the guidelines of the Society for Cardiovascular Pathology in 4 degrees: 0 = normal, 1 = mild, 2 = moderate, and 3 = severe.[10,11] Representative images are shown in Figure 2, *B*.

Gene Expression Analysis

Total RNA was isolated using QIAzol followed by miRNeasy Kit (Qiagen, Hilden, Germany). Details regarding isolation of total RNA are shown in the Online Data Supplement. Reverse transcription of RNA was carried out using the High-Capacity cDNA Kit (Life Technologies, Carlsbad,

histologic variables (inflammation, atherosclerosis, elastin fragmentation, CMN, and fibrosis) were semiquantitatively evaluated. *P* values < .05 are considered as significant and marked with an *asterisk*. Although differences between outer and inner curvatures were more pronounced with respect to atherosclerosis and CMN than fibrosis, the majority of patients with AR and even more patients with AS had no differences (*blue* bar). In a few patients, a tendency of increased scores in the outer curvature was detected and reached significant levels for elastin fragmentation. In the group of patients with AR, paired comparison of unadjusted histologic data was performed between outer and inner curvatures using the Stuart–Maxwell test. The corresponding contingency table is shown in Figure E6. The percentage of patients with no difference between outer and inner curvatures is plotted in *blue*, the percentage of patients with increased histologic scores in the outer curvature is plotted in *red* and in *green* in the inner curvature. *CI,* Confidence interval; *AR,* aortic regurgitation; *AD,* aortic diameter; *AS,* aortic stenosis; *CMN,* cystic medial necrosis.

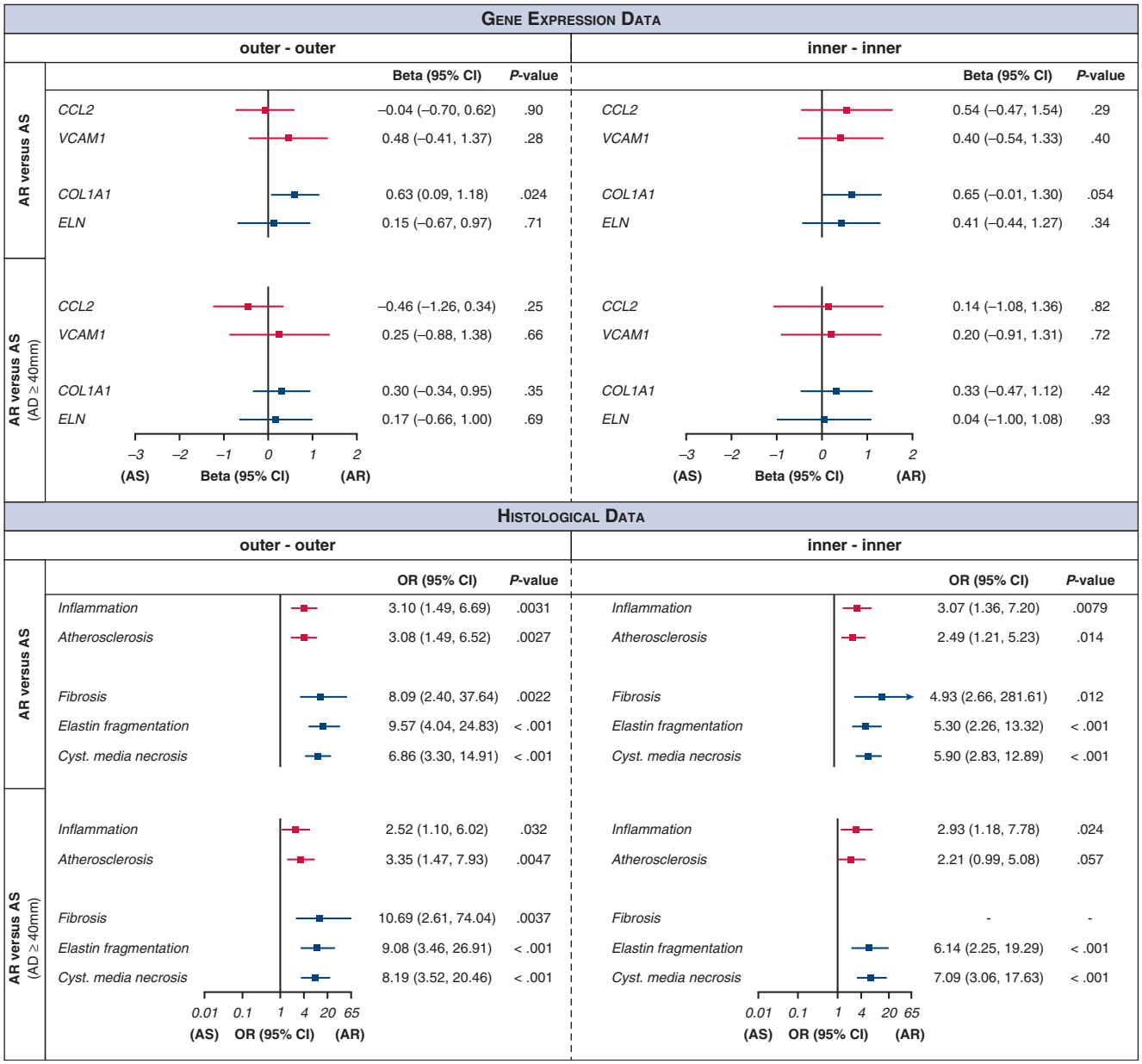

FIGURE 3. Comparison between all patients with AR and patients with AS and further refined by AD 40 mm or greater (comparison 1a and 1b). Gene expression of patients with AR (n = 64) were compared with gene expression of patients with AS (n = 67) and further refined by AD 40 mm or greater (AR, n = 58/AS, n = 44). The comparison of the outer curvatures is shown on the left and of the inner curvatures on the right. Comparison of log-transformed gene expression was performed using linear regression adjusted for age and sex. The regression coefficient beta is plotted as forest plots for genes associated with inflammation (red) or medial degeneration (blue). The comparison of histologic data of the outer curvatures is shown on the left and of the inner curvatures on the right. Comparison was performed using proportional odds regressions adjusted for age and sex. The odds ratio is plotted as forest plots for histologic parameter associated with inflammation (red) or medial degeneration (blue). In some cases, the model could not be computed because of lack of variability in the histologic score (eg, most values being equal to 0). *AR,* Aortic regurgitation; *AS,* aortic stenosis; *CI,* confidence interval; *AD,* aortic diameter; *OR,* odds ratio.

Calif), and resulting cDNA was finally used for real-time polymerase chain reaction as described in the Online Data Supplement.

Statistical Analysis

Adjusted comparisons of gene expression between different groups of patients were done using linear regression. Adjusted comparisons of histologic scores between different groups of individuals were done similarly but exchanging linear regression by the proportional odds model. Further details are provided in the Online Data Supplement.

RESULTS

Characteristics of the Study Cohort

As shown in Table 1, comparison of all patients with AR with all patients with AS revealed no differences in sex,

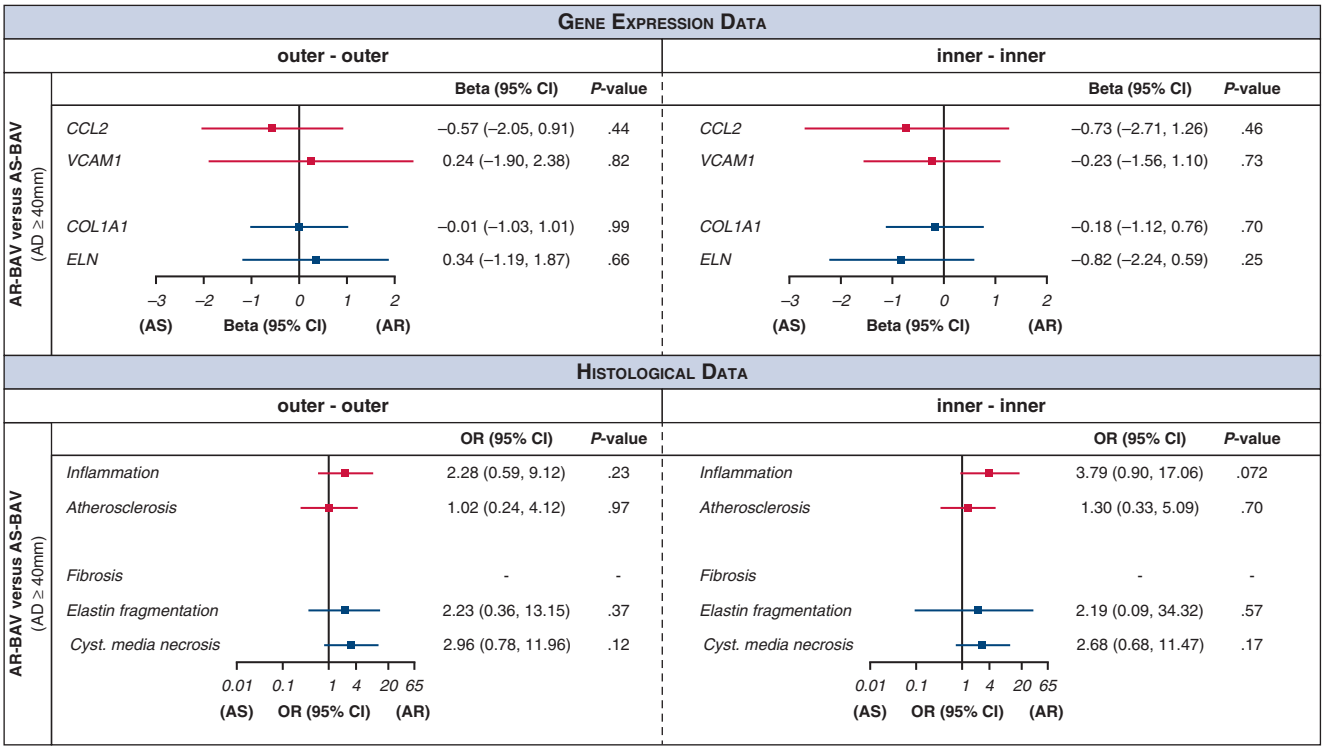

FIGURE 4. Comparison of patients with BAVs between patients with AR and patients with AS with AD 40 mm or greater (comparison 2). Gene expressions of patients with AR with an AD 40 mm or greater and BAV (AR-BAV, n = 18) were compared with gene expressions of patients with AS with an AD 40 mm or greater and BAV (AS-BAV, n = 40). The comparison of the outer curvatures is shown on the left and of the inner curvatures on the right. Comparison of log-transformed gene expression was performed using linear regression adjusted for age and sex. The regression coefficient beta is plotted as forest plots for genes associated with inflammation (red) or medial degeneration (blue). The comparison of histologic data of the outer curvatures is shown on the left and of the inner curvatures on the right. Comparison was performed using proportional odds regressions adjusted for age and sex. The odds ratio is plotted as forest plots for histologic parameter associated with inflammation (red) or medial degeneration (blue). In some cases, the model could not be computed because of lack of variability in the histologic score (eg, most values being equal to 0). *AR,* Aortic regurgitation; *AS,* aortic stenosis; *AD,* aortic diameter; *CI,* confidence interval; *OR,* odds ratio.

body mass index, and age. Furthermore, the most relevant comorbidities were similarly distributed in both groups. Significant differences were found regarding valve morphology and maximal cross-sectional proximal AD. As expected, patients with AS revealed a higher incidence of BAVs (33% vs 88%; $P < .001$) and exhibited a smaller AD (median, 52.0 vs 43.0; $P < .001$) compared with patients with AR (comparison 1a).

To reduce the effects of different AD, the study cohort was further refined by applying the cutoff for AD 40 mm or greater (comparison 1b). Consequently, the difference of AD between patients with AR and patients with AS was reduced but remained significantly different (median, 52.5 vs 47.5; $P < .001$).

Next, to exclude effects of different valve morphologies, BAVs were used to compare patients with AR and patients with AS (comparison 2). Patients with AR-BAV were significantly younger than patients with AS-BAV (median, 51.0 vs 63.0; $P < .001$), but AD was no longer significantly different (median, 51.0 vs 48.5; $P < .052$).

To investigate the effects of the different valve morphologies, BAVs and TAVs were compared within the AR group (comparison 3). No significant difference in AD between AR-BAV and AR-TAV was detected (median, 51.0 vs 53.0; $P = .46$), whereas the patients with AR-BAV were significantly younger (median = 51.0 vs 61.0 years; $P = .002$).

Negligible Differences Between Outer and Inner Curvature Within One Patient

To uncover differences between outer and inner curvature, paired samples were compared separately for each subgroup defined in Figure 1. Gene expression data, adjusted for age and sex, revealed no differences between the outer and inner curvatures. In Figure 2, *A*, the 2 subgroups, defined for comparison 1b, are depicted. The analyses of the other subgroups are presented in Figures E2, *A*, E3, *A*, and E4, *A*.

Histologic data for inflammation, atherosclerosis, elastin fragmentation, CMN, and fibrosis were scored to compare outer and inner curvatures (Figure 2, *C*). Because of the

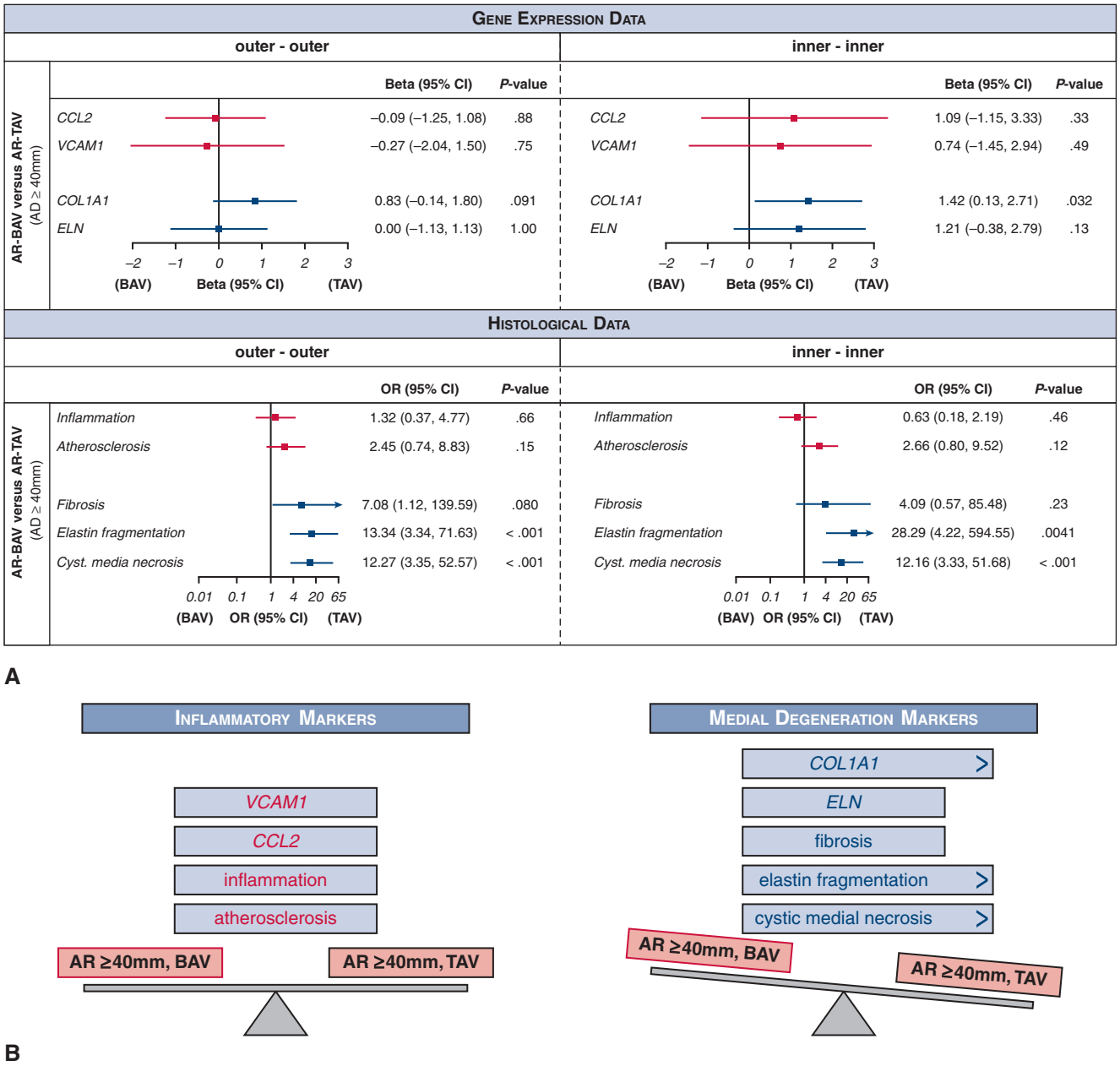

A

B

FIGURE 5. Comparison between TAV and BAV morphologies of patients with AR with AD 40 mm or greater (comparison 3). A, Gene expression between TAV and BAV morphologies of patients with AR with an AD 40 mm or greater were compared (AR-BAV, n = 18/AR-TAV, n = 40). The comparison of the outer curvatures is shown on the left and of the inner curvatures on the right. Comparison of log-transformed gene expression was performed using linear regression adjusted for age and sex. The regression coefficient beta is plotted as forest plots for genes associated with inflammation (red) or medial degeneration (blue). The comparison of histologic data of the outer curvatures is shown on the left and of the inner curvatures on the right. Comparison was performed using proportional odds regressions adjusted for age and sex. The odds ratio is plotted as forest plots for histologic parameter associated with inflammation (red) or medial degeneration (blue). B, The inflammatory markers (*red*) were similar in both subgroups. However, markers for medial degeneration (*blue*) were significantly higher in the AR-TAV compared with the AR-BAV subgroup. *AR,* Aortic regurgitation; *AD,* aortic diameter; *CI,* confidence interval; *BAV,* bicuspid aortic valve; *TAV,* tricuspid aortic valve; *OR,* odds ratio.

lack of variability of these score differences and model sample size, numeric problems were encountered in some cases when fitting age and adjusted models, and these results are not presented. For all subgroups, contingency tables were produced displaying the distribution of score differences (Figures E5-E8). In the majority of patients, scores did not differ between inner and outer curvatures. In a few patients, a tendency of increased scores in the outer curvature was

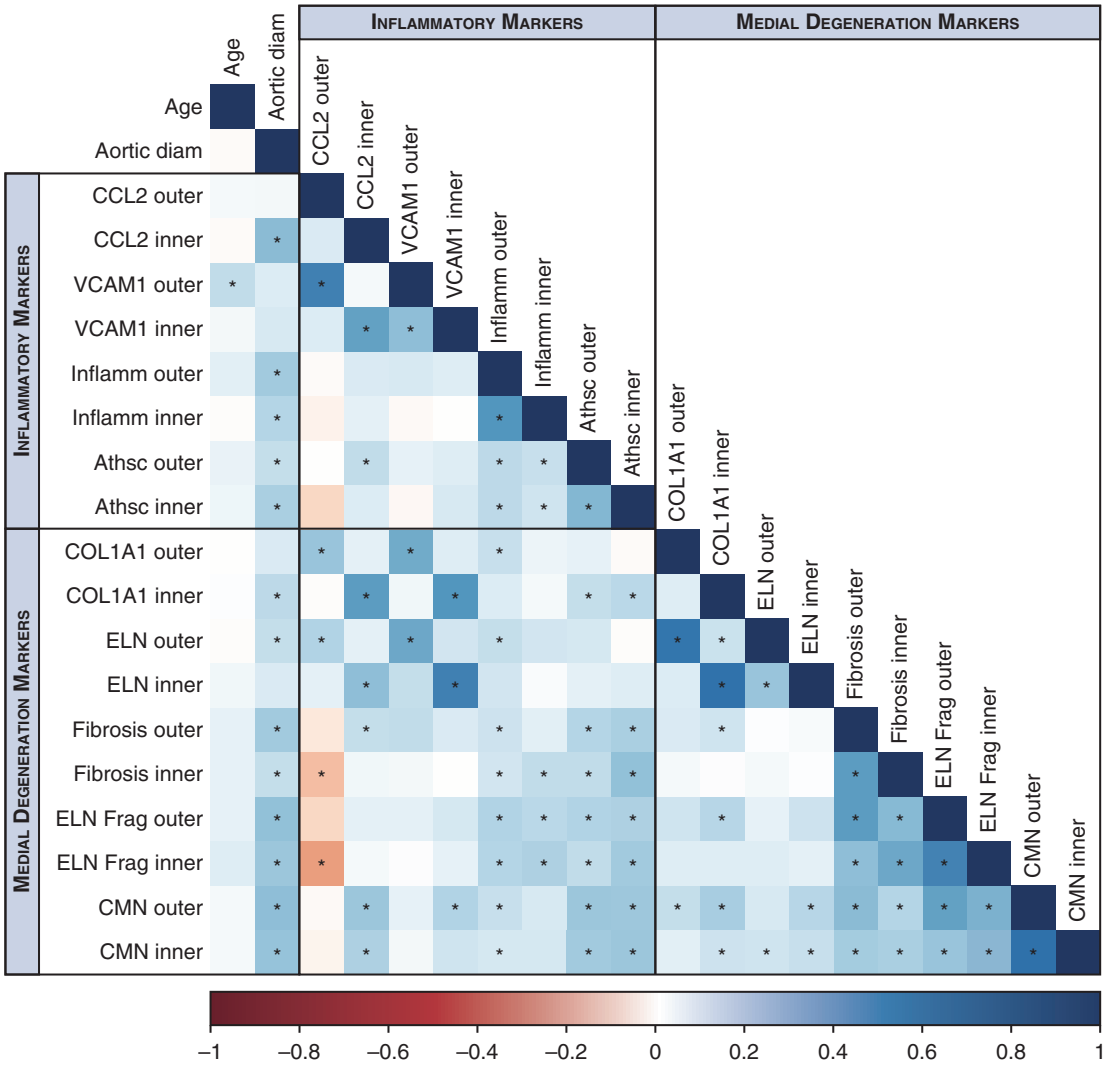

FIGURE 6. Correlogram representing Spearman correlations between inflammatory markers and medial degeneration markers for all individuals. Color indicates whether the correlation is positive (blue) or negative (red). The intensity of the color is proportional to the correlation coefficients. Correlations with a $P < .05$ are considered as significant and marked with an asterisk.

detected and reached significant levels for elastin fragmentation in the subgroup of patients with AR and patients with AR-TAV (Figure 2, *C* and Figures E2, *B*, and E4, *B*).

Slightly Increased Markers for Inflammation and Strongly Increased Markers for Medial Degeneration in Patients With Aortic Regurgitation (Comparison 1a and 1b)

As shown in Figure 3, gene expression and histologic scores of all patients with AR were compared with all patients with AS (comparison 1a) and subsequently further refined by AD 40 mm or greater (comparison 1b). Both comparisons were performed for outer and inner curvatures, separately. Comparing all patients without restriction regarding AD, gene expression of *CCL2* and *VCAM1* revealed no difference, whereas inflammatory markers using histology were increased in patients with AR. With respect to markers for medial degeneration, gene expression of *COL1A1* was slightly increased and histologic data were strongly increased in patients with AR. The subsequent refinement led to similar results except that gene expression of *COL1A1* was no longer different between those with AR and those with AS. It is not clear whether the gene expression of *COL1A1* is dependent on AD or there is not enough power to detect differences because of the reduced sample size in this subgroup.

No Differences Between Patients With Aortic Regurgitation and Patients With Aortic Stenosis With Bicuspid Aortic Valve Morphology (Comparison 2)

Study cohort of comparison 1b was further refined by BAV morphology leading to comparison 2 (AR-BAV vs AS-BAV). Neither gene expression nor histologic scores revealed significant differences between both subgroups (Figure 4).

MIS

Aortic Regurgitation With Tricuspid Valves Reveal More Severe Medial Degeneration than With Bicuspid Valves (Comparison 3)

By using the study cohort of comparison 1b, the impact of different valve morphologies was assessed leading to comparison 3 (AR-BAV vs AR-TAV). As depicted in Figure 5, data concerning inflammation displayed no differences between TAV and BAV morphology. Regarding markers for medial degeneration, gene expression of *COL1A1* was significantly increased in patients with AR-TAV in the inner curvature, whereas on the histologic level, fibrosis was not significantly different but tended toward higher expression in patients with AR-TAV. Of note, elastin fragmentation and CMN were highly increased in patients with AR-TAV compared with patients with AR-BAV.

Spearman Correlations Between Inflammatory and Medial Degeneration Markers in All Individuals

Inflammatory and medial degeneration markers were correlated to age and AD. Except for *VCAM1* gene expression, no correlation was found for age, whereas 5 of 8 inflammatory and 8 of 10 medial degeneration markers revealed significant positive correlations with AD.

Next, we correlated the different inflammatory and medial degeneration markers, and generally observed positive correlations. Between the different inflammatory markers, 36% revealed significant positive correlations, and 60% of significant positive correlations were found to correlate with the different medial degeneration makers. We observed 46% significant positive correlations between inflammation and medial degeneration markers (Figure 6). As shown in Figure E9, further correlograms were also computed for both subgroups of comparison 3.

DISCUSSION

Our results indicate that the proximal aorta in patients with AR showed an increased inflammation and medial degeneration compared with patients with AS. We further refined both groups by valve morphology. By comparing patients with bicuspid valves, patients with AR-BAV were significantly younger than patients with AS-BAV, but no further differences were identified. However, when comparing valve morphology within the subgroup of patients with AR, AR-TAV revealed increased markers for medial degeneration, but no differences regarding inflammatory markers compared with AR-BAV.

Aortic Regurgitation Exhibited Increased Markers for Inflammation and Medial Degeneration Compared With Aortic Stenosis

A previous MRI-based study revealed that patients with AS have more severe WSS in the outer curvature of the proximal aorta.[12] In contrast, a regurgitant aortic valve is associated with retrograde diastolic aortic flow leading to a disturbed flow pattern accompanied by lower WSS.[5,13] On the basis of these flow differences, we decided to compare the vascular remodeling between patients with AR and patients with AS. The histologic and gene analysis demonstrated more inflammation and medial degeneration in patients with AR. As reported by others,[14] aortopathy in regurgitation was characterized by more severe aortic dilation compared with stenosis. We also observed that AD positively correlates with inflammation and medial degeneration markers. Therefore, we subsequently refined both study groups by AD 40 mm or greater, excluding 34% of patients with AS but only 9% of patients with AR. The new refined analysis by AD 40 mm or greater confirmed our initial results regarding inflammation and medial degeneration in patients with AR.

Several studies reported that low WSS induces the expression of proinflammatory genes, thereby accelerating inflammation.[9,15-17] The aortic tissue of patients with AR revealed more inflammation, which may lead to activation of matrix metalloproteinases and subsequent elastin fragmentation, which in turn causes replacement of elastic fibers with a fibrocollagenous extracellular matrix.[18,19] These structural alterations lead to a weakening of aortic wall integrity and loss of aortic elasticity, which may further progress to aortic dilation.[1,20,21] Although hemodynamic alterations may influence the progression of aortic dilation in patients with AR, congenital factors may contribute.[22] This theory is supported by the fact that aortic dilation can also occur or progress after aortic valve surgery.[23,24]

Younger Age but No Histologic Differences in Bicuspid Aortic Regurgitation Versus Stenosis

Regarding valve morphology, we compared both aortic dysfunctional BAV subgroups. As in other studies,[24-27] patients with AR-BAV were significantly younger than patients with AS-BAV. Age- and sex-adjusted data revealed no differences in histologic or gene expression levels between both subgroups. A possible explanation for these results lies in the fact that all patients with BAV experience increased WSS over many years, which is further aggravated by a valve dysfunction as reported by Shan and colleagues[28] and Atkins and Sucosky.[29] Although both subgroups showed similar aortic wall alterations, it is extremely important to highlight that patients with AR-BAV were significantly younger, indicating that aortic remodeling in patients with AR-BAV occurs faster than in patients with AS-BAV. Wang and colleagues[24] reported that patients with AR-BAV demonstrated a faster proximal aorta dilation rate and identified AR in patients with BAV as a risk factor with increased hazard ratio.

Younger Age but Less Medial Degeneration in Bicuspid Aortic Regurgitation Versus Tricuspid Aortic Regurgitation

In the AR group, patients with BAV were younger than patients with TAV, which is in line with other studies.[30,31] This gap could be explained by a faster dilation rate in AR-BAV than in AR-TAV.[24,32] Of note, children with BAV already have an enlarged AD at birth compared with children with TAV.[33] Therefore, age plays a central role in aneurysm formation in patients with BAV and constitutes a major risk factor.[32]

Despite similar inflammation between both subgroups, makers for medial degeneration were more pronounced in patients with AR-TAV. It was previously reported that medial degeneration was more severe in patients with trileaflet aortic valve than bicuspid valve with an AD between 4 and 5 cm.[34] This marked degenerative medial differences could be due to an undiagnosed connective tissue disease in the patients with AR-TAV at the time of the surgery.

Study Limitations

Because of the small number of patients with AS-TAV, the comparison between TAV and BAV could not be performed within the AS group. Furthermore, relevant chemical parameters related to inflammation, such as lactate dehydrogenase or hemoglobin A1c, and detailed hemodynamic data, such as ejection fraction, degree of valve dysfunction, and aortic valve gradient, were not available. Furthermore, other hemodynamic factors (eg, transvalvular gradients, systolic aortic valve orifice area, left ventricle function) may have an additional impact on aortic wall changes, and a multivariate regression model incorporating complete clinical dataset would be appreciated. Nonetheless, most of the analyzed patients had normal systolic left ventricular function and transvalvular gradients in the AR cohort were negligible. Although the pathologists who read the sections were blinded, intraobserver variability was not reported.

CONCLUSIONS

Our results indicate that the proximal aorta in patients with AR showed an increased inflammation and medial degeneration compared with patients with AS. This suggests that disturbed transvalvular flow patterns, accompanied by lower WSS in the proximal aorta, may trigger severe remodeling regarding the aortic wall microstructure in patients with AR. On the basis of these findings, we should consider regurgitation as a risk factor for proximal aortic dilation. To confirm this conclusion, larger multicenter studies should be performed that give us deeper insights into disease progression. Now, we are conducting prospective studies to evaluate the value of specific circulating biomarkers that can be used to predict the progression of aortic disease. Furthermore, we are collecting longitudinal data on MRI-based transvalvular flow patterns in patients with AS and AR.

Conflict of Interest Statement

Authors have nothing to disclose with regard to commercial support.

The authors thank Mareile Schröder for her excellent technical assistance.

References

1. Hiratzka LF, Bakris GL, Beckman JA, Bersin RM, Carr VF, Casey DE Jr, et al. 2010 ACCF/AHA/AATS/ACR/ASA/SCA/SCAI/SIR/STS/SVM guidelines for the diagnosis and management of patients with Thoracic Aortic Disease: a report of the American College of Cardiology Foundation/American Heart Association Task Force on Practice Guidelines, American Association for Thoracic Surgery, American College of Radiology, American Stroke Association, Society of Cardiovascular Anesthesiologists, Society for Cardiovascular Angiography and Interventions, Society of Interventional Radiology, Society of Thoracic Surgeons, and Society for Vascular Medicine. *Circulation*. 2010;121:e266-369.
2. Folkersen L, Wagsater D, Paloschi V, Jackson V, Petrini J, Kurtovic S, et al. Unraveling divergent gene expression profiles in bicuspid and tricuspid aortic valve patients with thoracic aortic dilatation: the ASAP study. *Mol Med*. 2011;17:1365-73.
3. Kim HW, Stansfield BK. Genetic and epigenetic regulation of aortic aneurysms. *Biomed Res Int*. 2017;2017:7268521.
4. Maleki S, Bjorck HM, Folkersen L, Nilsson R, Renner J, Caidahl K, et al. Identification of a novel flow-mediated gene expression signature in patients with bicuspid aortic valve. *J Mol Med (Berl)*. 2013;91:129-39.
5. Martufi G, Forneris A, Appoo JJ, Di Martino ES. Is there a role for biomechanical engineering in helping to elucidate the risk profile of the thoracic aorta? *Ann Thorac Surg*. 2016;101:390-8.
6. Lindsay ME, Dietz HC. The genetic basis of aortic aneurysm. *Csh Perspect Med*. 2014;4:a015909.
7. van Ooij P, Markl M, Collins JD, Carr JC, Rigsby C, Bonow RO, et al. Aortic valve stenosis alters expression of regional aortic wall shear stress: new insights from a 4-dimensional flow magnetic resonance imaging study of 571 subjects. *J Am Heart Assoc*. 2017;6.
8. Ando J, Yamamoto K. Vascular mechanobiology: endothelial cell responses to fluid shear stress. *Circ J*. 2009;73:1983-92.
9. Bjorck HM, Renner J, Maleki S, Nilsson SF, Kihlberg J, Folkersen L, et al. Characterization of shear-sensitive genes in the normal rat aorta identifies Hand2 as a major flow-responsive transcription factor. *PLoS One*. 2012;7:e52227.
10. Halushka MK, Angelini A, Bartoloni G, Basso C, Batoroeva L, Bruneval P, et al. Consensus statement on surgical pathology of the aorta from the Society for Cardiovascular Pathology and the Association For European Cardiovascular Pathology: II. Noninflammatory degenerative diseases - nomenclature and diagnostic criteria. *Cardiovasc Pathol*. 2016;25:247-57.
11. Stone JR, Bruneval P, Angelini A, Bartoloni G, Basso C, Batoroeva L, et al. Consensus statement on surgical pathology of the aorta from the Society for Cardiovascular Pathology and the Association for European Cardiovascular Pathology: I. Inflammatory diseases. *Cardiovasc Pathol*. 2015;24:267-78.
12. Youssefi P, Gomez A, He T, Anderson L, Bunce N, Sharma R, et al. Patient-specific computational fluid dynamics-assessment of aortic hemodynamics in a spectrum of aortic valve pathologies. *J Thorac Cardiovasc Surg*. 2017;153:8-20.e23.
13. Reimold SC, Maier SE, Aggarwal K, Fleischmann KE, Piwnica-Worms D, Kikinis R, et al. Aortic flow velocity patterns in chronic aortic regurgitation: implications for Doppler echocardiography. *J Am Soc Echocardiogr*. 1996;9:675-83.
14. Falk V, Baumgartner H, Bax JJ, De Bonis M, Hamm C, Holm PJ, et al. 2017 ESC/EACTS Guidelines for the management of valvular heart disease. *Eur J Cardiothorac Surg*. 2017;52:616-64.
15. Chiu JJ, Chien S. Effects of disturbed flow on vascular endothelium: pathophysiological basis and clinical perspectives. *Physiol Rev*. 2011;91:327-87.
16. Nayak L, Lin Z, Jain MK. "Go with the flow": how Kruppel-like factor 2 regulates the vasoprotective effects of shear stress. *Antioxid Redox Signal*. 2011;15:1449-61.

17. Dhawan SS, Avati Nanjundappa RP, Branch JR, Taylor WR, Quyyumi AA, Jo H, et al. Shear stress and plaque development. *Expert Rev Cardiovasc Ther*. 2010;8:545-56.
18. Anidjar S, Dobrin PB, Eichorst M, Graham GP, Chejfec G. Correlation of inflammatory infiltrate with the enlargement of experimental aortic aneurysms. *J Vasc Surg*. 1992;16:139-47.
19. Maiellaro K, Taylor WR. The role of the adventitia in vascular inflammation. *Cardiovasc Res*. 2007;75:640-8.
20. Azadani AN, Chitsaz S, Mannion A, Mookhoek A, Wisneski A, Guccione JM, et al. Biomechanical properties of human ascending thoracic aortic aneurysms. *Ann Thorac Surg*. 2013;96:50-8.
21. Fedak PW, de Sa MP, Verma S, Nili N, Kazemian P, Butany J, et al. Vascular matrix remodeling in patients with bicuspid aortic valve malformations: implications for aortic dilatation. *J Thorac Cardiovasc Surg*. 2003;126:797-806.
22. Tadros TM, Klein MD, Shapira OM. Ascending aortic dilatation associated with bicuspid aortic valve: pathophysiology, molecular biology, and clinical implications. *Circulation*. 2009;119:880-90.
23. Padang R, Bannon PG, Jeremy R, Richmond DR, Semsarian C, Vallely M, et al. The genetic and molecular basis of bicuspid aortic valve associated thoracic aortopathy: a link to phenotype heterogeneity. *Ann Cardiothorac Surg*. 2013;2:83-91.
24. Wang Y, Wu B, Li J, Dong L, Wang C, Shu X. Impact of aortic insufficiency on ascending aortic dilatation and adverse aortic events after isolated aortic valve replacement in patients with a bicuspid aortic valve. *Ann Thorac Surg*. 2016;101:1707-14.
25. Al-Atassi T, Hynes M, Sohmer B, Lam BK, Mesana T, Boodhwani M. Aortic root geometry in bicuspid aortic insufficiency versus stenosis: implications for valve repair. *Eur J Cardiothorac Surg*. 2015;47:e151-4.
26. Benedik J, Dohle DS, Wendt D, Pilarczyk K, Price V, Mourad F, et al. Comparison of ascending aortic cohesion between patients with bicuspid aortic valve stenosis and regurgitation. *Eur J Cardiothorac Surg*. 2014;46:e89-93.
27. Girdauskas E, Rouman M, Disha K, Fey B, Dubslaff G, von Kodolitsch Y, et al. Morphologic and functional markers of aortopathy in patients with bicuspid aortic valve insufficiency versus stenosis. *Ann Thorac Surg*. 2017;103:49-57.
28. Shan Y, Li J, Wang Y, Wu B, Barker AJ, Markl M, et al. Aortic shear stress in patients with bicuspid aortic valve with stenosis and insufficiency. *J Thorac Cardiovasc Surg*. 2017;153:1263-72.e1.
29. Atkins SK, Sucosky P. Etiology of bicuspid aortic valve disease: focus on hemodynamics. *World J Cardiol*. 2014;6:1227-33.
30. Agnese V, Pasta S, Michelena HI, Mina C, Romano GM, Carerj S, et al. Patterns of ascending aortic dilatation and predictors of surgical replacement of the aorta: a comparison of bicuspid and tricuspid aortic valve patients over eight years of follow-up. *J Mol Cell Cardiol*. 2019;135:31-9.
31. Ren X, Li F, Wang C, Hou Z, Gao Y, Yin W, et al. Age- and sex-related aortic valve dysfunction and aortopathy difference in patients with bicuspid aortic valve. *Int Heart J*. 2019;60:637-42.
32. Cozijnsen L, Braam RL, Waalewijn RA, Schepens MA, Loeys BL, van Oosterhout MF, et al. What is new in dilatation of the ascending aorta? Review of current literature and practical advice for the cardiologist. *Circulation*. 2011;123:924-8.
33. Siu SC, Silversides CK. Bicuspid aortic valve disease. *J Am Coll Cardiol*. 2010;55:2789-800.
34. Heng E, Stone JR, Kim JB, Lee H, MacGillivray TE, Sundt TM. Comparative histology of aortic dilatation associated with bileaflet versus trileaflet aortic valves. *Ann Thorac Surg*. 2015;100:2095-101.

Key Words: aortic hemodynamic, aortic regurgitation, aortic remodeling, aortic stenosis, aortopathy, bicuspid aortic valve, tricuspid aortic valve

MIS

000 Comparison of microstructural alterations in the proximal aorta between aortic stenosis and regurgitation

Tatiana M. Sequeira Gross, MD, Diana Lindner, PhD, Francisco M. Ojeda, PhD, Johannes Neumann, MD, Nimrat Grewal, MD, Thomas Kuntze, MD, Stefan Blankenberg, MD, Hermann Reichenspurner, MD, PhD, Dirk Westermann, MD, and Evaldas Girdauskas, MD, Hamburg and Bad Berka, Germany; and Leiden, The Netherlands

Compared with stenosis, aortic tissue from patients with regurgitation revealed increased inflammation and even more medial degeneration, which was aggravated in patients with tricuspid valve morphology.

Supplementary Material

Comparison of microstructural alterations in the proximal aorta between aortic stenosis and regurgitation

Tatiana M. Sequeira Gross, MD[1*], Diana Lindner, PhD[2,3*], Francisco M. Ojeda, PhD[2], Johannes Neumann, MD[2,3], Nimrat Grewal, MD[4], Thomas Kuntze, MD[5], Stefan Blankenberg, MD[2,3], Hermann Reichenspurner, MD, PhD[1,3], Dirk Westermann, MD[2,3*], and Evaldas Girdauskas, MD[1,3*]

[1]Clinic for Cardiovascular Surgery, University Heart and Vascular Center Hamburg, Hamburg, Germany

[2]Clinic for Cardiology, University Heart and Vascular Center Hamburg, Hamburg, Germany

[3]DZHK (German Center for Cardiovascular Research), partner site Hamburg/Kiel/Lübeck

[4]Clinic of Cardiovascular Surgery, Leiden University Medical Center, Leiden, Netherlands

[5]Clinic of Cardiac Surgery, Central Hospital Bad Berka, Bad Berka, Germany

* Both authors contributed equally

2 Material and methods

2.2 Aortic tissue samples based on MRI

The maximal flow jet contact area was determined individually for each patient based on the MRI results. The aortic samples were obtained by following the next steps as depicted in Figure E1. First, in order to guide the surgeon to a precise collection of the aortic specimens (jet sample and non-jet sample), we subdivided the circumference of the proximal aorta into six segments. Secondly, steady-state free precession (SSFP) MRI images were acquired to visually identify the turbulent flow jet in stenotic or regurgitant aortic valves. Using the SSFP images, we determined the area of the proximal aorta exposed to the maximal flow-jet, as well as the "low flow" contralateral area. Two full-thickness aortic wall specimens were obtained. Third, once the jet direction and the aortic segment was defined, the exact distance (cm) between aortic valve plane and the area of maximal flow-induced stress in the proximal aorta was measured, in order to perform the aortotomy. Finally, in patients in whom a jet was not visualized, the aortic samples were obtained from standard aortotomy prior to closure of the aorta.

2.3 Histopathological analysis

Aortic samples were fixed in neutral-buffered formalin for at least 48 hours at room temperature. After routine processing for paraffin embedding, aortic samples were sectioned perpendicular to the aortic wall. Sections were stained with hematoxylin-eosin (H&E) to evaluate inflammation and atherosclerosis as well as resorcin fuchsin straining to assess elastin fragmentation (ELN frag). Using MOVAT's pentachrome, fibrosis and cystic media necrosis was determined[1]. Two blinded, experienced pathologist evaluated all aortic specimens.

2.4 Gene expression analysis

Tissue samples taken from 131 patients were immediately snap frozen in liquid nitrogen and stored at -80°C until further processing. To isolate total RNA, tissue was disrupted between two 7mm stainless steel beads using the TissueLyser II (Qiagen). Before starting, the adapter was cooled and tubes were loaded with 700 µl QIAzol lysis reagent (Qiagen) and beads. Immediately after adding the frozen tissue into the QIAzol, samples were placed in the TissueLyser II and shaken at high speed with an oscillation frequency of $30s^{-1}$ for five min. To prevent warming of the samples, both adapter and samples were cooled down before repeating the vigorous shaking additional three times.

Subsequently, 590 µl water and 10 µl proteinase K (>600mAU/ml, Qiagen) were added and incubated for 30 min at 55°C for digestion. Further, samples were supplemented with 140 µl chloroform, mixed by vigorous shaking for approximately 1 min and incubated for 2-3 min at room temperature. To separate the RNA-containing phase, samples were centrifuged for 15 min at 12,000g at 4°C. The upper phase was kept and supplemented with 1.5-fold volume of absolute ethanol. To purify the RNA, miRNeasy Kit was used according to manufacturer's instructions. Therefore, samples were transferred to the RNeasy columns and washed once. To eliminate genomic DNA, DNase I solution (Qiagen) was added and incubated at least 15 min at room temperature for digestion. Columns were washed several times before eluting the RNA in 30 µl water. RNA concentration was determined using the Nanodrop 2000c spectrophotometer and RNA was stored at -80°C for further processing.

To assess gene expression for target genes (*CCL2*: chemokine (C-C motif) ligand 2; *COL1A1*: collagen type I, alpha 1; *VCAM1*: vascular cell adhesion protein 1; *ELN*: elastin), real-time PCR was performed using 5 µl gene expression master mix (Life Technologies) and 0.5 µl gene

expression assay (*CCL2*: Hs00234140_m1; *COL1A1*: Hs00164004_m1; *VCAM1*: Hs00365485_m1; *ELN*: Hs00355783_m1; Life Technologies, USA). Gene expression assays include forward and reverse primers as well the FAM-labeled probe. As template, 1 µl of cDNA was used in a final volume of 10 µl. Each sample was analyzed in duplicates. Furthermore, the gene expression of *18S* (Hs99999901_s1) was used as endogenous control to normalize the data using the formula $2^{-\Delta Ct}$ and plotted as x-fold to *18S* as absolute gene expression. The real-time PCR was carried out on a 7900 TaqMan system using SDS v2.4 (Applied Biosystems, USA).

2.5 Statistical analysis

Continuous variables were presented using quartiles and binary variables using absolute and relative frequencies. Baseline characteristics were compared with help of the Mann-Whitney test for continuous variables and Fisher's exact test for categorical variables. Spearman correlations were computed for selected variables. Adjusted comparisons of gene expression between different groups of patients were done using linear regression. The log-transformed gene expression was the dependent variable and the independent variable of interest was a group indicator (that is, a variable that is equal to 1 when and individual belongs to a group and 0 otherwise). These models were adjusted for age and sex. Adjusted comparisons of histological scores between different groups of individuals were done in a similar fashion as for the gene expression but exchanging linear regression by the proportional odds model. Paired comparisons of gene expression between outer and inner curvature were done using an age and sex adjusted linear mixed model. The log-transformed gene expression was the dependent variable and the independent variable of interest was an outer curvature indicator (i.e. a variable that is 1 for outer gene expression and 0 otherwise). To take into account the correlation between outer and inner measurements the linear mixed model

included a random intercept per patient. To perform age and sex adjusted paired comparisons between outer and inner curvature histological scores similar mixed models were used substituting the linear mixed models by proportional odds models. Additionally paired unadjusted comparisons were performed using the Stuart-Maxwell test.

Statistical methods were implemented in R statistical software version 3.6.1 (R Core Team 2019, Vienna, Austria). Unadjusted histological data from the contingency table were plotted using Graph Pad Prism 6.05 (San Diego, USA).

3 Results

3.2 Negligible differences between outer and inner curvature within one patient.

As described in Figure 1, several comparisons were performed by refining the study cohorts by aortic diameter and valve morphology. The results for all subgroups used for the different comparisons are shown in the Figures E2 to E8.

3.6 Spearman correlations between inflammatory markers and medial degeneration for both subgroups of comparison 3.

First inflammatory markers and markers for medial degeneration were correlated to age and aortic diameter. In the AR-TAV group, mainly makers for medial degeneration are positively correlated to AD. This was not the case in the AR-BAV group.

Overall, the AR-BAV group revealed inconsistent correlation, whereas in the AR-TAV group inflammatory markers and markers for medial degeneration were mainly positively correlated.

References

1. Grewal N, Girdauskas E, DeRuiter M, Goumans MJ, Poelmann RE, Klautz RJM, et al. The role of hemodynamics in bicuspid aortopathy: a histopathologic study. *Cardiovasc Pathol.* 2019;41:29-37.

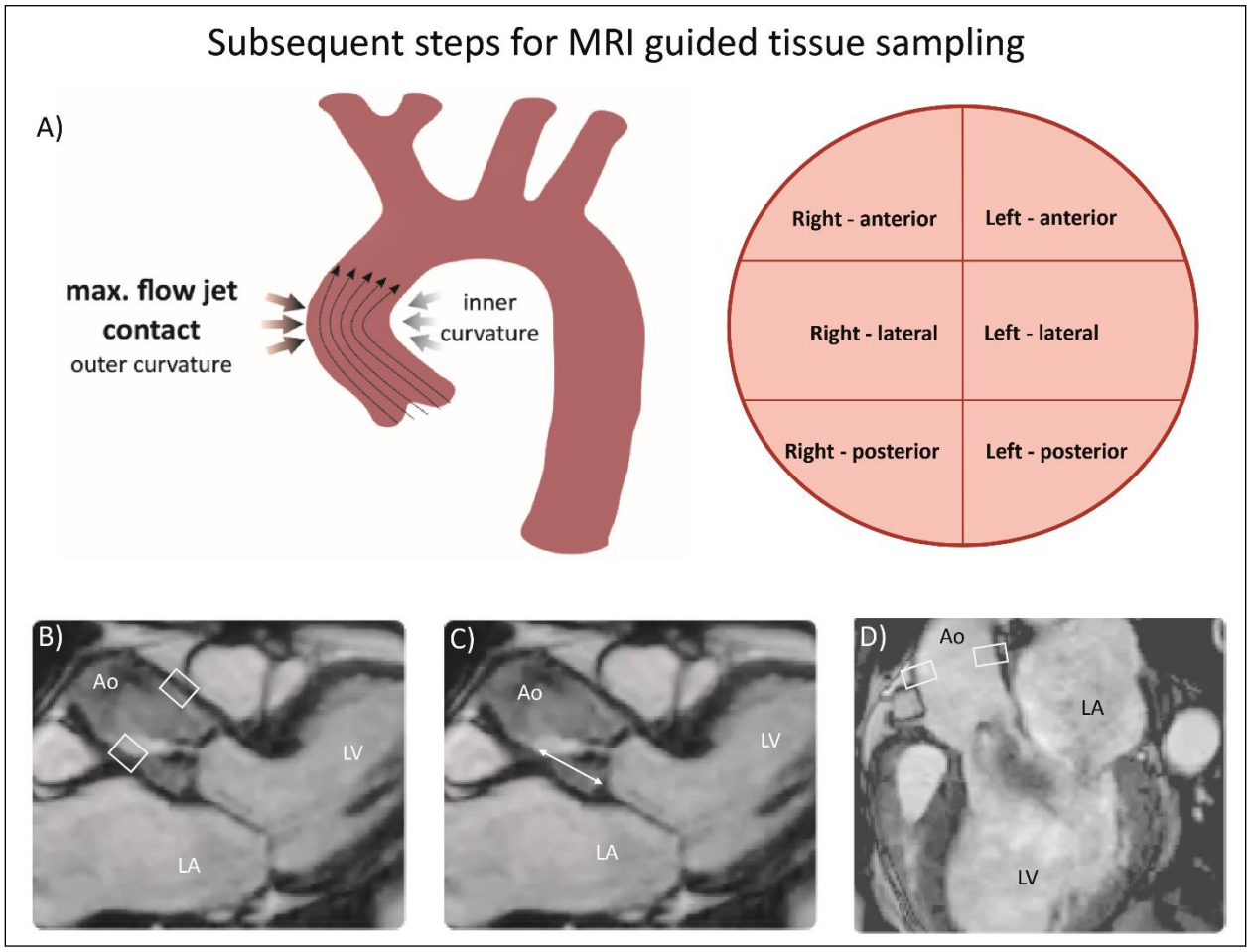

Figure E1: Steps for MRI-guided tissue sampling. A) Representative demonstration of the six segments of the proximal aorta. B) With the SSFP images we were able to define the jet sample and the non-jet sample area. Both areas were demarked with a white square. C) The aortotomy height (represented by the white arrow), was defined as the distance (cm) between aortic valve plane and the area of maximal flow-induced stress in the proximal aorta. D) In patients in whom a jet was not visualized, the aortic samples were obtained from standard aortotomy height prior to closure of the aorta. The whites squares demarcated the area where the two samples were obtain.

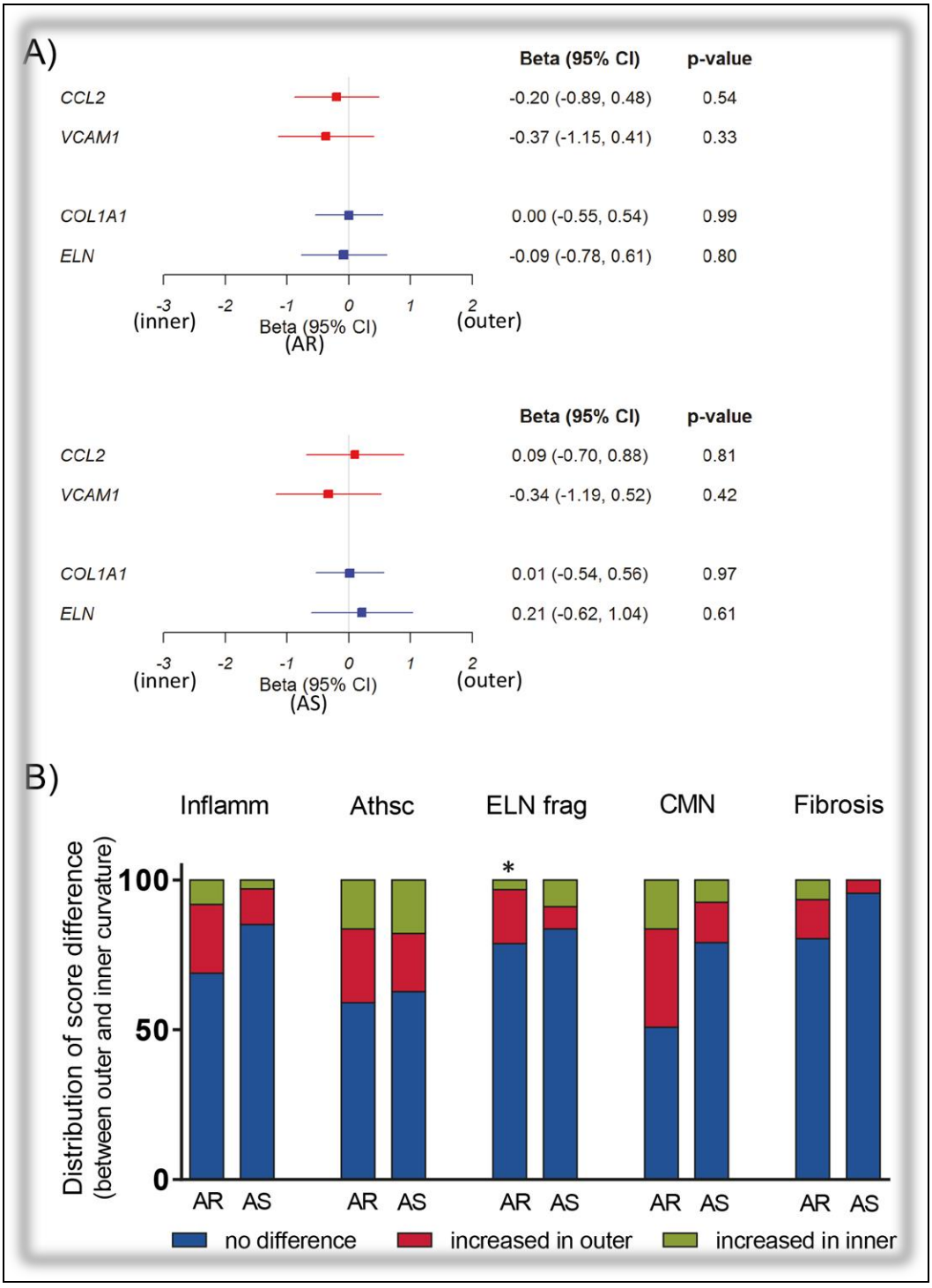

Figure E2: Study cohort of comparison 1a – Difference between outer and inner curvature for each individual patient. A) Gene expression of AR-patients (n = 64) and AS-patients (n = 67) of the outer curvature for *CCL2*, *VCAM1*, *COL1A1* and *ELN* was compared to the gene expression

of the respective inner curvature from the same patient. No differences were detected between outer and inner curvature. Paired comparison of log transformed gene expression between outer and inner curvature was performed using a linear mixed model adjusted for age and sex. The regression coefficient beta is plotted as forest plots for genes associated with inflammation (red) and for genes associated with medial degeneration (blue).

B) The majority of AR-patients and even more AS-patients revealed no differences between outer and inner curvature for all five histological variables inflammation (Inflamm), atherosclerosis (Athsc), elastin fragmentation (ELN frag), cystic medial necrosis (CMN) and fibrosis (blue bar). In very few patients, a tendency of increased scores in the outer curvature was detected and reached significance for ELN fragmentation in the group of AR-patients.

Unadjusted paired comparison for histological data between outer and inner curvature was performed using the Stuart-Maxwell test. The corresponding contingency table is shown in Figure E5. The percentage of patients with no difference between outer and inner curvature is plotted in blue, the percentage of patients with increased histological scores in the outer curvature is plotted in red and in green with increased histological scores in the inner curvature. In some cases the model could not be computed because of lack of variability in the histological score (e.g. most values being equal to 0).

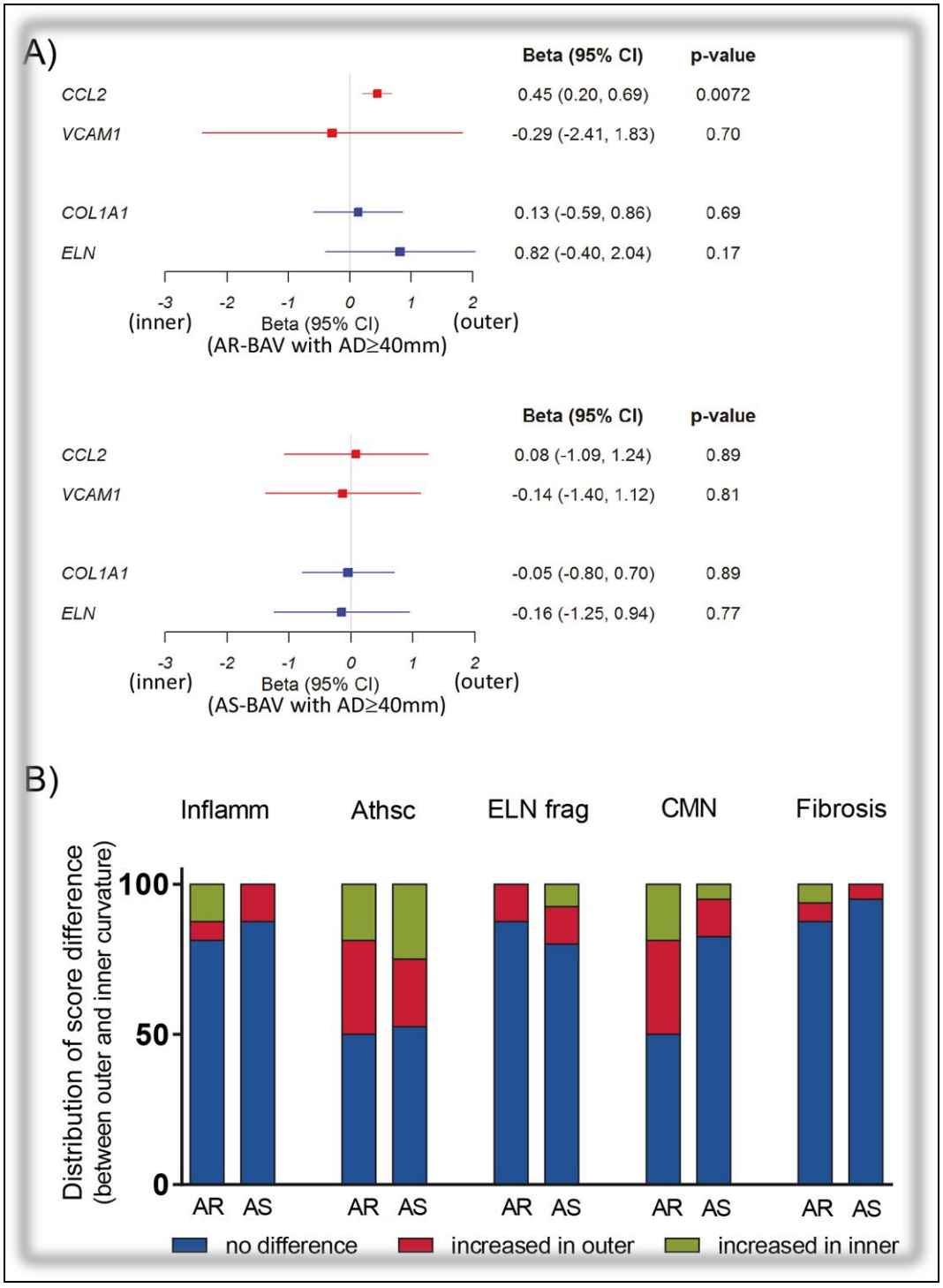

Figure E3: Study cohort of comparison 2 – Difference between outer and inner curvature for each individual patient. A) Gene expression of AR-BAV-patients with AD ≥40mm (n = 18) and AS-BAV-patients with AD ≥ 40mm (n = 40) of the outer curvature for *CCL2*, *VCAM1*,

COL1A1 and *ELN* was compared to the gene expression of the respective inner curvature from the same patient. CCL2 expression was higher in the outer curvature of AR-BAV- patients. Paired comparison of log transformed gene expression between outer and inner curvature was performed using a linear mixed model adjusted for age and sex. The regression coefficient beta is plotted as forest plots for genes associated with inflammation (red) and for genes associated with medial degeneration (blue).

B) The majority of AR-BAV-patients and AS-BAV-patients revealed no differences between outer and inner curvature for all five histological variables inflammation (Inflamm), atherosclerosis (Athsc), elastin fragmentation (ELN frag), cystic medial necrosis (CMN) and fibrosis (blue bar). In very few patients, a tendency of increased scores in the outer curvature but did not reach significant levels.

Unadjusted paired comparison for histological data between outer and inner curvature was performed using the Stuart-Maxwell test. The corresponding contingency table is shown in Figure E7. The percentage of patients with no difference between outer and inner curvature is plotted in blue, the percentage of patients with increased histological scores in the outer curvature is plotted in red and in green with increased histological scores in the inner curvature.

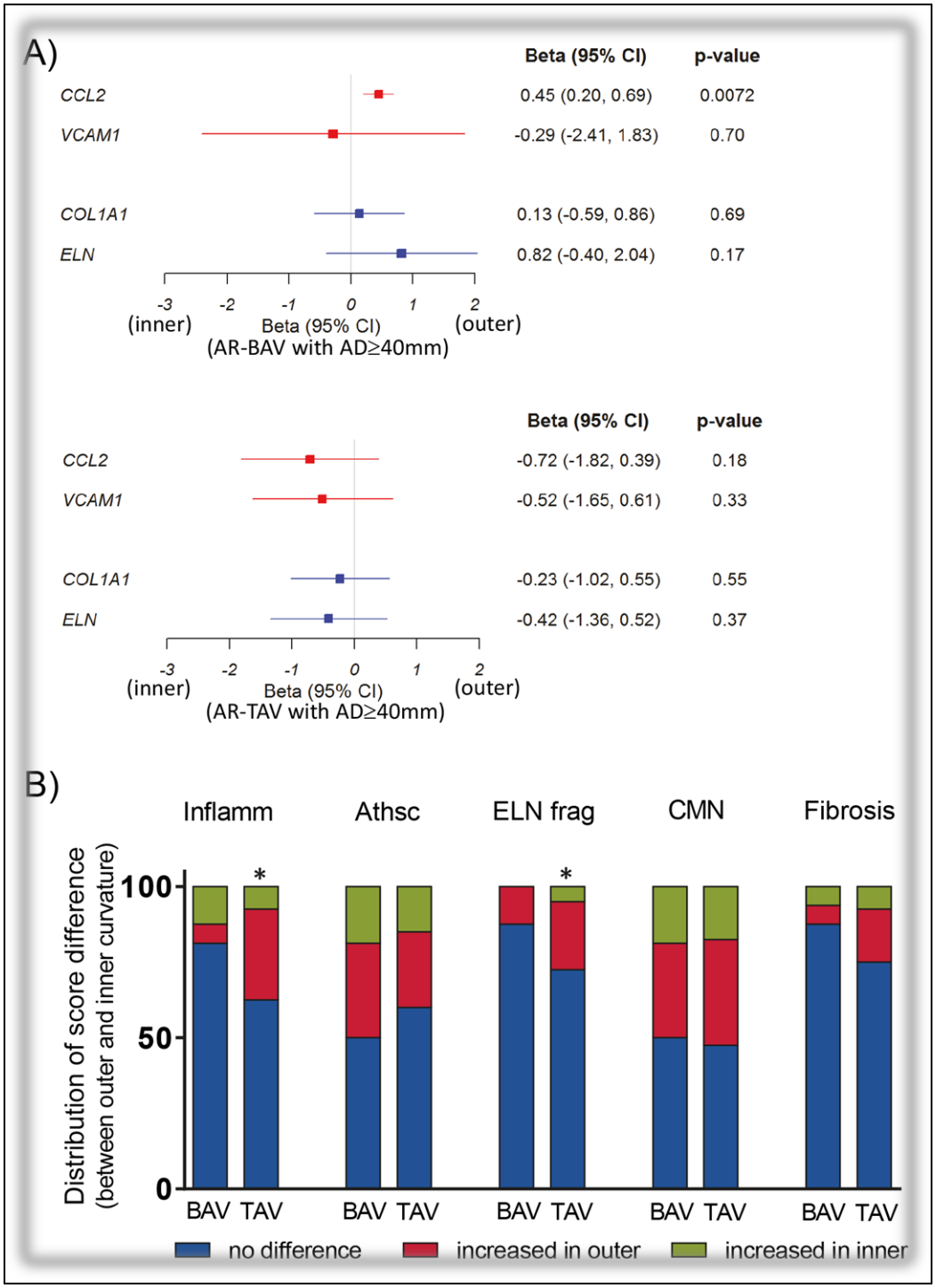

Figure E4: Study cohort of comparison 3 – Difference between outer and inner curvature for each individual patient. A) Gene expression of AR-BAV-patients with AD ≥40mm (n = 18) and AR-TAV-patients with AD ≥40mm (n = 40) of the outer curvature for *CCL2*, *VCAM1*,

COL1A1 and *ELN* was compared to the gene expression of the respective inner curvature from the same patient. CCL2 expression was higher in the outer curvature of AR-BAV- patients. Paired comparison of log transformed gene expression between outer and inner curvature was performed using a linear mixed model adjusted for age and sex. The regression coefficient beta is plotted as forest plots for genes associated with inflammation (red) and for genes associated with medial degeneration (blue).

B) The majority of AR-BAV-patients and AR-TAV-patients revealed no differences between outer and inner curvature for all five histological variables inflammation (Inflamm), atherosclerosis (Athsc), elastin fragmentation (ELN frag), cystic medial necrosis (CMN) and fibrosis (blue bar). In very few patients, a tendency of increased scores in the outer curvature was detected and reached significant levels for Inflamm and ELN frag in the group of AR-TAV-patients.

Unadjusted paired comparison for histological data between outer and inner curvature were performed using the Stuart-Maxwell test. The corresponding contingency table is shown in Figure E8. The percentage of patients with no difference between outer and inner curvature is plotted in blue, the percentage of patients with increased histological scores in the outer curvature is plotted in red and in green with increased histological scores in the inner curvature.

Histologic differences between outer and inner curvature (comparision 1a)

Aortic regurgitation, AR, n = 64

Inflammation (p = 0.18)		increased in inner curvature				
		0	1	2	3	Sum
increased in outer curvature	0	40.98	4.92	1.64	0	8.2
	1	18.03	24.59	1.64	0	
	2	1.64	1.64	3.28	0	
	3	0	0	1.64	0	
	Sum	22.95				68.85

Atherosclerosis (p = 0.76)		increased in inner curvature				
		0	1	2	3	Sum
increased in outer curvature	0	32.79	11.48	1.64	0	16.4
	1	14.75	18.03	1.64	1.64	
	2	1.64	6.56	8.2	0	
	3	0	1.64	0	0	
	Sum	24.59				59.02

Elastin fragmentation (p = 0.036)		increased in inner curvature				
		0	1	2	3	Sum
increased in outer curvature	0	45.9	1.64	1.64	0	3.28
	1	4.92	8.2	0	0	
	2	1.64	0	1.64	0	
	3	8.2	3.28	0	22.95	
	Sum	18.04				78.69

Cyst. medial necrosis (p = 0.21)		increased in inner curvature				
		0	1	2	3	Sum
increased in outer curvature	0	13.11	3.28	0	0	16.4
	1	6.56	16.39	8.2	1.64	
	2	1.64	9.84	3.28	3.28	
	3	0	4.92	9.84	18.03	
	Sum	32.8				50.81

Fibrosis (p = 0.23)		increased in inner curvature				
		0	1	2	3	Sum
increased in outer curvature	0	70.49	4.92	0	0	6.56
	1	13.11	8.2	0	0	
	2	0	0	1.64	1.64	
	3	0	0	0	0	
	Sum	13.11				80.33

Aortic stenosis AS, n = 67

Inflammation (p = 0.13)		increased in inner curvature				
		0	1	2	3	Sum
increased in outer curvature	0	68.66	2.99	0	0	2.99
	1	7.46	14.93	0	0	
	2	4.48	0	1.49	0	
	3	0	0	0	0	
	Sum	11.94				85.08

Atherosclerosis (p = 1.00)		increased in inner curvature				
		0	1	2	3	Sum
increased in outer curvature	0	49.25	16.42	0	0	17.91
	1	17.91	11.94	0	1.49	
	2	0	1.49	1.49	0	
	3	0	0	0	0	
	Sum	19.4				62.68

Elastin fragmentation (p = 1.00)		increased in inner curvature				
		0	1	2	3	Sum
increased in outer curvature	0	77.61	8.96	0	0	8.96
	1	7.46	4.48	0	0	
	2	0	0	0	0	
	3	0	0	0	1.49	
	Sum	7.46				83.58

Cyst. medial necrosis (p = 0.19)		increased in inner curvature				
		0	1	2	3	Sum
increased in outer curvature	0	29.85	5.97	0	0	7.46
	1	7.46	49.25	0	0	
	2	1.49	4.48	0	1.49	
	3	0	0	0	0	
	Sum	13.43				79.1

Fibrosis (p = 0.50)		increased in inner curvature				
		0	1	2	3	Sum
increased in outer curvature	0	95.52	0	0	0	0
	1	2.99	0	0	0	
	2	0	1.49	0	0	
	3	0	0	0	0	
	Sum	4.48				95.52

Figure E5: Contingency table for both study cohorts of comparison 1a – Difference between outer and inner curvature for each individual patient. The five histological variables inflammation, atherosclerosis, elastin fragmentation, cystic medial necrosis and fibrosis were determined in the inner and outer curvature of each individual patient using semi-quantitative scores (0 = normal, 1 = mild, 2 = moderate and 3 = severe). ELN frag in the AR-patients was significantly differently increased in the outer curvature compared to the respective inner curvature. In Figure E2B, sum of percentage with no differences between outer and inner are plotted as blue bars. While the sum of the percentage of patients with increased histological scores in the outer curvature is plotted in red and increased histological scores in the inner curvature in green.

Histologic differences between outer and inner curvature (comparision 1b)

Aortic regurgitation, AR (AD ≥40mm), n = 58

Inflammation (p = 0.26)		increased in inner curvature			
	0	1	2	3	Sum
0	37.5	5.36	1.79	0	8.94
1	17.86	26.79	1.79	0	
2	1.79	1.79	3.57	0	
3	0	0	1.79	0	
Sum	23.23				67.86

increased in outer curvature

Atherosclerosis (p = 0.73)		increased in inner curvature			
	0	1	2	3	Sum
0	28.57	10.71	1.79	0	16.08
1	16.07	19.64	1.79	1.79	
2	1.79	7.14	8.93	0	
3	0	1.79	0	0	
Sum	26.79				57.14

increased in outer curvature

Elastin fragmentation (p = 0.036)		increased in inner curvature			
	0	1	2	3	Sum
0	42.86	1.79	1.79	0	3.58
1	5.36	7.14	0	0	
2	1.79	0	1.79	0	
3	8.93	3.57	0	25	
Sum	19.65				76.79

increased in outer curvature

Cyst. medial necrosis (p = 0.30)		increased in inner curvature			
	0	1	2	3	Sum
0	8.93	3.57	0	0	17.86
1	7.14	16.07	8.93	1.79	
2	0	10.71	3.57	3.57	
3	0	5.36	10.71	19.64	
Sum	33.92				48.21

increased in outer curvature

Fibrosis (p = 0.23)		increased in inner curvature			
	0	1	2	3	Sum
0	67.86	5.36	0	0	7.15
1	14.29	8.93	0	0	
2	0	0	1.79	1.79	
3	0	0	0	0	
Sum	14.29				78.58

increased in outer curvature

Aortic stenosis AS (AD ≥40mm), n = 44

Inflammation (p = 0.064)		increased in inner curvature			
	0	1	2	3	Sum
0	65.91	0	0	0	0
1	6.82	18.18	0	0	
2	6.82	0	2.27	0	
3	0	0	0	0	
Sum	13.64				86.36

increased in outer curvature

Atherosclerosis (p = 1.00)		increased in inner curvature			
	0	1	2	3	Sum
0	40.91	22.73	0	0	25
1	20.45	11.36	0	2.27	
2	0	0	2.27	0	
3	0	0	0	0	
Sum	20.45				54.54

increased in outer curvature

Elastin fragmentation (p = 1.00)		increased in inner curvature			
	0	1	2	3	Sum
0	75	9.09	0	0	9.09
1	11.36	2.27	0	0	
2	0	0	0	0	
3	0	0	0	2.27	
Sum	11.36				79.54

increased in outer curvature

Cyst. medial necrosis (p = 1.00)		increased in inner curvature			
	0	1	2	3	Sum
0	29.55	2.27	0	0	4.54
1	6.82	54.55	0	0	
2	0	4.55	0	2.27	
3	0	0	0	0	
Sum	11.37				84.1

increased in outer curvature

Fibrosis (p = 1.00)		increased in inner curvature			
	0	1	2	3	Sum
0	95.45	0	0	0	0
1	4.55	0	0	0	
2	0	0	0	0	
3	0	0	0	0	
Sum	4.55				95.45

increased in outer curvature

Figure E6: Contingency table for both study cohorts of comparison 1b – Difference between outer and inner curvature for each individual patient. The five histological variables inflammation, atherosclerosis, elastin fragmentation, cystic medial necrosis and fibrosis were determined in the inner and outer curvature of each individual patient using semi-quantitative scores (0 = normal, 1 = mild, 2 = moderate and 3 = severe). ELN frag in the AR-patients was significantly differently increased in the outer curvature compared to the respective inner curvature. In Figure 2C of the main manuscript, sum of percentage with no differences between outer and inner are plotted as blue bars. While the sum of the percentage of patients with increased histological scores in the outer curvature is plotted in red and increased histological scores in the inner curvature in green.

Histologic differences between outer and inner curvature (comparision 2)

Aortic regurgitation & Bicuspid, AR-BAV (AD ≥40mm), n = 18

Inflammation (p = 1.00)		increased in inner curvature			
	0	1	2	3	Sum
0	43.75	12.5	0	0	12.5
1	6.25	37.5	0	0	
2	0	0	0	0	
3	0	0	0	0	
Sum	6.25				81.25

(increased in outer curvature)

Atherosclerosis (p = 0.61)		increased in inner curvature			
	0	1	2	3	Sum
0	43.75	18.75	0	0	18.75
1	18.75	6.25	0	0	
2	0	12.5	0	0	
3	0	0	0	0	
Sum	31.25				50

(increased in outer curvature)

Elastin fragmentation (p = 0.50)		increased in inner curvature			
	0	1	2	3	Sum
0	81.25	0	0	0	0
1	12.5	6.25	0	0	
2	0	0	0	0	
3	0	0	0	0	
Sum	12.5				87.5

(increased in outer curvature)

Cyst. medial necrosis (p = 1.00)		increased in inner curvature			
	0	1	2	3	Sum
0	18.75	12.5	0	0	18.75
1	18.75	25	6.25	0	
2	0	12.5	0	0	
3	0	0	0	6.25	
Sum	31.25				50

(increased in outer curvature)

Fibrosis (p = 1.00)		increased in inner curvature			
	0	1	2	3	Sum
0	87.5	6.25	0	0	6.25
1	6.25	0	0	0	
2	0	0	0	0	
3	0	0	0	0	
Sum	6.25				87.5

(increased in outer curvature)

Aortic stenosis & Bicuspid, AS-BAV (AD ≥40mm), n = 40

Inflammation (p = 0.12)		increased in inner curvature			
	0	1	2	3	Sum
0	70	0	0	0	0
1	7.5	15	0	0	
2	5	0	2.5	0	
3	0	0	0	0	
Sum	12.5				87.5

(increased in outer curvature)

Atherosclerosis (p = 1.00)		increased in inner curvature			
	0	1	2	3	Sum
0	40	22.5	0	0	25
1	22.5	10	0	2.5	
2	0	0	2.5	0	
3	0	0	0	0	
Sum	22.5				52.5

(increased in outer curvature)

Elastin fragmentation (p = 0.73)		increased in inner curvature			
	0	1	2	3	Sum
0	75	7.5	0	0	7.5
1	12.5	2.5	0	0	
2	0	0	0	0	
3	0	0	0	2.5	
Sum	12.5				80

(increased in outer curvature)

Cyst. medial necrosis (p = 0.38)		increased in inner curvature			
	0	1	2	3	Sum
0	30	2.5	0	0	5
1	7.5	52.5	0	0	
2	0	5	0	2.5	
3	0	0	0	0	
Sum	12.5				82.5

(increased in outer curvature)

Fibrosis (p = 0.50)		increased in inner curvature			
	0	1	2	3	Sum
0	95	0	0	0	0
1	5	0	0	0	
2	0	0	0	0	
3	0	0	0	0	
Sum	5				95

(increased in outer curvature)

Figure E7: Contingency table for both study cohorts of comparison 2 – Difference between outer and inner curvature for each individual patient. The five histological variables inflammation, atherosclerosis, elastin fragmentation, cystic medial necrosis and fibrosis were determined in the inner and outer curvature of each individual patient using semi-quantitative scores (0 = normal, 1 = mild, 2 = moderate and 3 = severe). No significant differences between outer and inner curvature was found. In Figure E3B, sum of percentage with no differences between outer and inner are plotted as blue bars. While the sum of the percentage of patients with increased histological scores in the outer curvature is plotted in red and increased histological scores in the inner curvature in green.

Histologic differences between outer and inner curvature (comparision 3)

Aortic regurgitation & Bicuspid, AR-BAV (AD ≥40mm), n = 18

Inflammation (p = 1.00)		increased in inner curvature				
		0	1	2	3	Sum
increased in outer curvature	0	43.75	12.5	0	0	12.5
	1	6.25	37.5	0	0	
	2	0	0	0	0	
	3	0	0	0	0	
	Sum	6.25				81.25

Atherosclerosis (p = 0.61)		increased in inner curvature				
		0	1	2	3	Sum
increased in outer curvature	0	43.75	18.75	0	0	18.75
	1	18.75	6.25	0	0	
	2	0	12.5	0	0	
	3	0	0	0	0	
	Sum	31.25				50

Elastin fragmentation (p = 0.50)		increased in inner curvature				
		0	1	2	3	Sum
increased in outer curvature	0	81.25	0	0	0	0
	1	12.5	6.25	0	0	
	2	0	0	0	0	
	3	0	0	0	0	
	Sum	12.5				87.5

Cyst. medial necrosis (p = 1.00)		increased in inner curvature				
		0	1	2	3	Sum
increased in outer curvature	0	18.75	12.5	0	0	18.75
	1	18.75	25	6.25	0	
	2	0	12.5	0	0	
	3	0	0	0	6.25	
	Sum	31.25				50

Fibrosis (p = 1.00)		increased in inner curvature				
		0	1	2	3	Sum
increased in outer curvature	0	87.5	6.25	0	0	6.25
	1	6.25	0	0	0	
	2	0	0	0	0	
	3	0	0	0	0	
	Sum	6.25				87.5

Aortic regurgitation & Tricuspid, AR-TAV (AD ≥40mm), n = 40

Inflammation (p = 0.032)		increased in inner curvature				
		0	1	2	3	Sum
increased in outer curvature	0	35	2.5	2.5	0	7.5
	1	22.5	22.5	2.5	0	
	2	2.5	2.5	5	0	
	3	0	0	2.5	0	
	Sum	30				62.5

Atherosclerosis (p = 0.86)		increased in inner curvature				
		0	1	2	3	Sum
increased in outer curvature	0	22.5	7.5	2.5	0	15
	1	15	25	2.5	2.5	
	2	2.5	5	12.5	0	
	3	0	2.5	0	0	
	Sum	25				60

Elastin fragmentation (p = 0.048)		increased in inner curvature				
		0	1	2	3	Sum
increased in outer curvature	0	27.5	2.5	2.5	0	5
	1	2.5	7.5	0	0	
	2	2.5	0	2.5	0	
	3	12.5	5	0	35	
	Sum	22.5				72.5

Cyst. medial necrosis (p = 0.28)		increased in inner curvature				
		0	1	2	3	Sum
increased in outer curvature	0	5	0	0	0	17.5
	1	2.5	12.5	10	2.5	
	2	0	10	5	5	
	3	0	7.5	15	25	
	Sum	35				47.5

Fibrosis (p = 0.18)		increased in inner curvature				
		0	1	2	3	Sum
increased in outer curvature	0	60	5	0	0	7.5
	1	17.5	12.5	0	0	
	2	0	0	2.5	2.5	
	3	0	0	0	0	
	Sum	17.5				75

Figure E8: Contingency table for both study cohorts of comparison 3 – Difference between outer and inner curvature for each individual patient. The five histological variables inflammation, atherosclerosis, elastin fragmentation, cystic medial necrosis and fibrosis were determined in the inner and outer curvature of each individual patient using semi-quantitative scores (0 = normal, 1 = mild, 2 = moderate and 3 = severe). Significant differences between outer and inner curvature was found for inflamm and ELN frag in the AR-TAV group. In Figure E4B, sum of percentage with no differences between outer and inner are plotted as blue bars. While the sum of the percentage of patients with increased histological scores in the outer curvature is plotted in red and increased histological scores in the inner curvature in green.

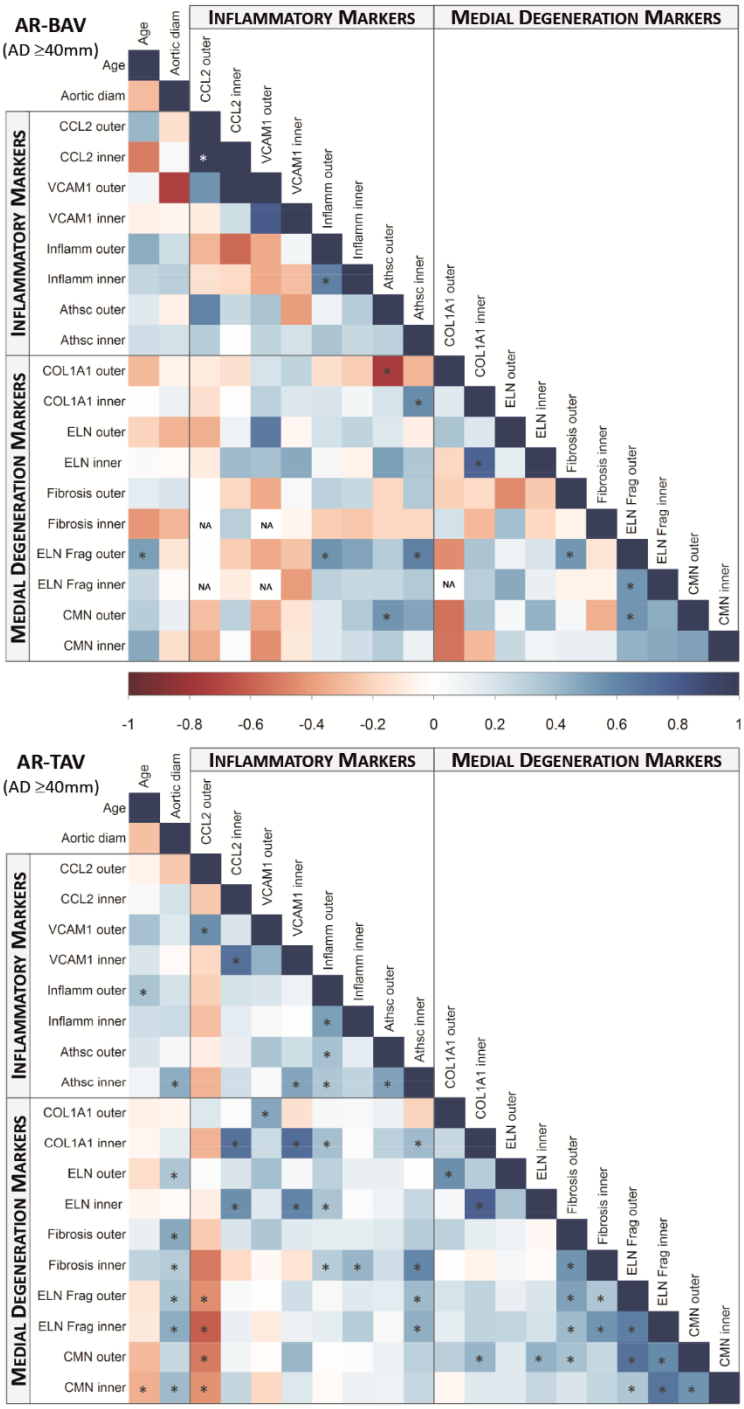

Figure E9: Correlogram representing Spearman correlations between inflammatory markers and medial degeneration markers for both subgroups of comparison 3. AR-BAV-patients with AD ≥40mm (n = 18) and AR-TAV-patients with AD ≥40mm (n = 40) were analyzed. Color indicates whether the correlation is positive (blue) or negative (red). The

intensity of the color is proportional to the correlation coefficients. Correlations with a p-value < 0.05 are considered as significant and were marked with an asterisk. Correlations that could not be computed are showed as NA. This occurred when one of the two variables that was being correlated turned out to be constant after removing the missing values in both variables (this could happen for the histological scores since they take at most 4 different values).

Comparison of microstructural alterations in the proximal aorta between aortic stenosis and regurgitation

2. Summary and description of paper

Abbreviations

AD = aortic diameter

AS = aortic stenosis

AR = aortic regurgitation

AVR = aortic valve replacement

BAV = bicuspid aortic valve

CCL2 = gene expression of chemokine (C-C motif) ligand 2

CMN = cystic medial necrosis

COL1A1 = gene expression of collagen type I, alpha 1

ECM = extracellular matrix

ELN = gene expression of elastin

MMP = matrix metalloproteinases

MRI = magnetic resonance imaging

LVOT = left ventricular outflow tract

SSFP = steady-state free precession

TAV = tricuspid aortic valve

VCAM1 = gene expression of vascular cell adhesion protein 1

WSS = wall shear stress

Introduction

The aorta is a complex organ with a unique structure. A healthy aortic wall is capable of resisting the pressure-induced cyclic forcing action on it [1]. This physiological function is mainly determined by the extracellular matrix component of the aortic wall [2]. Structural alterations caused by different mechanisms, such as detrimental hemodynamics or inherited disorders, lead to excessive dilation of the aortic diameter, so-called aortopathy or aneurysm [3-7]. Due to the frequently silent clinical course and an increased risk of life-threatening events, there is an urgent need for a better understanding of risk factors and pathophysiology of aortic dilation [8, 9]. Over the years, only a few aortic risk factor have been identified, including age, genetic predisposition, smoking, atherosclerosis, hypertension and bicuspid valve [3, 9-11].

Although aortic valve disease has not been yet classified as a risk factor in the guidelines, studies have shown that proximal aortopathy is commonly associated with a variable degree of aortic valve regurgitation (AR) or stenosis (AS) [11-13]. Based on our previous research, the presence of AR and aortopathy occurs mostly in younger patients aged between 30-60 years, more frequently male, and they tend to have a larger aortic diameter compared to AS patients [14-16]. Due to the larger cross-sectional aortic diameter, the risk for adverse aortic events (i.e., dissection or rupture) tends to be significantly higher [17, 18]. On the other hand, aortopathy with AS occurs in an older population, between 65-70 years, and is often related to the presence of a bicuspid valve [19-21]. The incidence of tricuspid aortic valve stenosis and aneurysm is rather low [22] .

Despite obvious differences in the clinical presentation of aortopathies between the AR vs. AS patients, to date, there are no comparative studies that address the underlying pathophysiological mechanisms responsible for above mentioned differences between AR vs. AS aortopathy. Therefore, we aimed to analyze the association among transvalvular flow patterns, histologic alterations in the aortic wall, and gene expression of the proximal aorta in patients with aortic valve regurgitation versus aortic stenosis. In order to identify the differences in aortic remodeling, age- and sex adjusted data for inflammation (*CCL2, VCAM1*, inflammation and atherosclerosis) and medial degeneration (*COL1A1, ELN*, fibrosis, elastin fragmentation, and cystic medial necrosis) were compared.

Material and Methods

Study population

A total of 131 consecutive patients who underwent elective aortic valve replacement (AVR) surgery with or without proximal aortic replacement between January 2012 through December 2016 at the Central Hospital, Bad Berka, Germany, were identified and served as the study population. All patients who underwent urgent surgical procedures (e.g., acute aortic dissection or endocarditis), as well as patients with previously known connective tissue disorders were excluded from this study.

Based on valve dysfunction (AR and AS) and valve morphology (BAV and TAV), several comparisons adjusted for age and sex were analyzed. First, in comparison-1a all AR-patients (n = 64) were compared to all AS-patients (n = 67). Secondly, in order to reduce the effects of different AD, the following comparisons were refined by applying the cutoff for AD ≥40 mm. In comparison-1b, AR-patients (n = 58) were compared to AS-patients (n = 44) refined by AD ≥40 mm. Comparison-2 used AR- and AS-patients refined by bicuspid aortic valve morphology and AD (AR-BAV, n = 18 and AS-BAV, n = 40). In comparison-3, AR-patients with bicuspid aortic valve (AR-BAV, n = 18) were compared to AR-patients with tricuspid aortic valve (AR-TAV, n = 40) (Figure 1, page 3).

Aortic tissue samples based on MRI

Steady-state free precession (SSFP) MRI images were acquired to visually identify the turbulent flow jet in stenotic or regurgitant aortic valves. Two full-thickness aortic wall specimens were obtained intraoperatively. One sample was obtained from the area of the proximal aorta exposed to the maximal flow-jet (jet sample), as identified by preoperative MRI, and the second sample from the contralateral or "low flow" area (non-jet sample).

Both aortic samples were divided for subsequent histological staining and gene expression analysis. Samples for histopathological analysis were fixed in neutral-buffered formalin, whereas samples for gene expression analysis were snap frozen in liquid nitrogen. Subsequent analysis was designed to evaluate inflammatory markers such as the endothelial adhesion molecule *VCAM1*, the chemo-attractive chemokine *CCL2* on gene expression level, as well as infiltrated

inflammatory cells and atherosclerosis on histological tissue sections. Furthermore, we focused on the medial degeneration markers. Therefore, we measured the gene expression of the extracellular proteins *COL1A1* and *ELN* and additionally fibrosis, elastin fragmentation (ELN frag) and cystic medial necrosis (CMN) on histological tissue sections (Figure 1, page 3).

Histopathological analysis

To evaluate inflammation and atherosclerosis, the aortic samples were stained with hematoxylin-eosin. Using MOVAT's pentachrome and resorcin fuchsin straining we were able to assess fibrosis, elastin fragmentation and cystic media necrosis [23]. The results of the histological analysis were semi-quantitatively graded by two experienced pathologist according to the guidelines of the Society for Cardiovascular Pathology [24, 25] (Figure 2B, page 4).

Gene expression analysis

Reverse transcription of RNA was carried out using the High-Capacity cDNA Kit (Life Technologies, USA). Therefore, 125 ng total RNA from tissue samples was reversely transcribed into cDNA. Resulting cDNA was further diluted to a final working concentration of 1.25 ng/µl. To assess gene expression for target genes, real-time PCR was performed using 5 µl gene expression master mix (Life Technologies) and 0.5 µl gene expression assay (Life Technologies, USA). As template, 1 µl of cDNA was used in a final volume of 10 µl. Each sample was analyzed in duplicates. Furthermore, the gene expression of *18S* was used as endogenous control to normalize the data using the formula $2^{-\Delta Ct}$ and plotted as x-fold to *18S* as absolute gene expression. The real-time PCR was carried out on a 7900 TaqMan system using SDS v2.4 (Applied Biosystems, USA).

Statistical analysis

Continuous variables were presented using quartiles and binary variables using absolute and relative frequencies. Spearman correlations were computed for selected variables and groups of patients. Adjusted comparisons of gene expression between different groups of patients were done using linear regression. The log-transformed gene expression was the dependent variable and the independent variable of interest was a group indicator (that is, a variable that is equal to 1 when and individual belongs to a group and 0 otherwise). These models were adjusted for age and sex.

Adjusted comparisons of histological scores between different groups of individuals were done in a similar fashion as for the gene expression but exchanging linear regression by the proportional odds model. Statistical methods were implemented in R statistical software version 3.6.1 (R Core Team 2019, Austria) and graphs were plotted using Graph Pad Prism 6.05 (San Diego, USA).

Results

Study population

As presented in table 1 of the manuscript, sex and BMI were similarly distributed in both groups, however AR patients tended to be younger than AS patients (mean age 59 vs. 61 years, $p = 0.058$). The maximal cross-sectional proximal aortic diameter was significantly larger in AR patients (median 52.0 vs. 43.0; $p < 0.001$) (comparison 1a). A total of 58 (90.6%) AR patients vs. 44 (65.7%) AS patients had a proximal aortic diameter ≥40 mm (comparison 1b).

In comparison 2, the AR-BAV patients were on average 12 years younger and had a tendency towards larger proximal aorta as compared to the AS–BAV patients (median 51.0 mm vs. 48.5 mm; $p = 0.052$). In comparison 3, maximal aortic diameter was comparable in AR-BAV vs. AR-TAV subgroups (median 51.0 mm vs. 53.0 mm, $p = 0.46$). However, the AR-BAV patients were a decade younger than AR-TAV patients (mean age 51 years vs. 61 years, $p = 0.002$) (Table 1, page 5).

Negligible differences between outer and inner curvature within one patient

Histological scores of the semi-quantitative analysis were compared between the outer an inner curvature of the same patient. To highlight the individual differences, we normalized the scores by subtracting the histological score of the inner curvature from the respective histological score of the outer curvature. The mean of calculated differences was plotted and revealed that elastin fragmentation was slightly increased in the outer curvature compared to its corresponding inner curvature in AR patients. Inflammation markers, CMN and fibrosis were similar in both curvatures within one patient (Figure 2C, page 4).

Slightly increased markers for inflammation and strongly increased markers for medial degeneration in AR-patients (comparison - 1a and 1b)

Histological scores and gene expression of all AR-patients were compared to all AS-patients (comparison 1a) and subsequently further refined by AD ≥40 mm (comparison 1b). Both comparisons were performed for outer and inner curvatures, separately. In comparison 1a, gene expression of *CCL2* and *VCAM1* revealed no difference, whereas inflammatory markers using histology were increased in AR-patients (Figure 3, page 6).

Regardless to medial degeneration markers, gene expression of *COL1A1* was slightly increased and histological data were strongly increased in AR-patients. The gene expression of *COL1A1* was not longer different between AR- and AS- after subsequent refinement by AD ≥40 mm. It is not clear whether, the gene expression of *COL1A1* dependent from AD or there is not enough power to detect differences because of the reduced sample size in this subgroup.

No differences between AR- and AS-patients with bicuspid aortic valve morphology (comparison - 2)

The correlation analysis performed between the pro-inflammatory as well as the medial degeneration gene markers revealed no significant difference between the AR-BAV vs. AS-BAV patients. There were no significant differences in all analyzed histological features between both study groups (Figure 4, page 7).

Aortic regurgitation with tricuspid valves reveals more severe medial degeneration than with bicuspid valves (comparison - 3)

In comparison 3 (AR-BAV vs. AR-TAV) neither gene expression nor histological data concerning inflammation displayed differences between TAV and BAV morphology. Regarding medial degeneration, the AR-TAV-patients showed a significantly higher gene expression of *COL1A1* in the inner curvature. However, on the histological analysis, fibrosis showed only a tendency towards higher expression in AR-TAV patients. Of note, ELN fragmentation and CMN were highly increased in AR-TAV-patients compared to AR-BAV-patients (Figure 5, page 8).

Spearman correlations between inflammatory and medial degeneration markers in all individuals

Except for *VCAM1* gene expression, no correlation was found for age, whereas 5 out of 8 inflammatory and 8 out of 10 medial degeneration markers revealed significant positive correlations with aortic diameter. Next, we correlated the different inflammatory markers with the medial degeneration markers and generally observed positive correlations.

Finally, we decided to correlate the inner and outer curvature in all patients. Between different inflammatory markers, 36% revealed significant positive correlations, whereas 60% significant positive correlations were found correlating the different medial degeneration makers (Figure 6, page 9).

Discussion

Our results demonstrated that patients with aortic regurgitation (AR) presented with an increased inflammation and medial degeneration in the proximal aorta compared to aortic stenosis (AS) patients. Furthermore, we performed subgroups analysis according to the valve morphology and the presence of aortopathy. By comparing patients with bicuspid valve, AR-BAV-patients were significantly younger compared to AS-BAV-patients, but no further differences were identified. However, when comparing valve morphology within the subgroup of AR-patients, we confirmed significantly more medial degeneration in aortic specimens resected from patients with AR-TAV than those with AR-BAV.

Aortic regurgitation exhibited increased markers for inflammation and medial degeneration compared to aortic stenosis (comparison 1a, 1b)

Shear stress exerts effects through various pathophysiological mechanisms depending on the kind and the magnitude of shear stress [26]. Previous MRI-based study revealed that AS patients have more severe WSS in the outer curvature of proximal aorta, predominantly due to the presence of a high velocity eccentric flow [27]. In contrast, regurgitant aortic valve is associated with retrograde

diastolic aortic flow leading to a turbulent flow pattern accompanied by lower WSS levels in the proximal aorta [7, 28]. Based on these flow differences, we decided to compare the vascular remodeling between patients with AR and patients with AS.

Our results confirmed that aortopathy in AR is characterized by younger patients' age and more severe aortic dilation as compared to AS. These different phenotypic features were also reported by other study groups [29]. Semiquantitative histological analysis of intraoperatively obtained aortic samples was performed and compared between both study groups. Regardless the type of aortic valve dysfunction, paired aortic samples (i.e., outer vs. inner curvature) revealed similar findings regarding inflammation and medial degeneration. However, the histological and gene comparison between both groups (comparison 1a) revealed that the AR group presented more severe inflammation and microstructural changes in the extracellular matrix (i.e., elastin fragmentation, fibrosis and CMN) as compared to the AS group. We additionally observed that aortic diameter positively correlates with inflammation and medial degeneration markers. Therefore, we stratified the groups by an aortic diameter >40 mm (comparison 1b) and were able to confirm that pro-inflammation and medial degeneration markers were still significantly higher expressed in the AR cohort.

Aortic regurgitation is characterized by recirculation eddies which lead to reduced WSS within the ascending aorta [7, 28]. Several previous studies reported that low WSS induces the expression of pro-inflammatory genes and thereby accelerates the inflammation [30-33]. Several endogenous factors were previously shown to instigate the immune response in the aortic wall resulting in a cascade of inflammatory events including activation of mononuclear inflammatory cells, matrix metalloproteinases (MMPs) and fibroblasts [34, 35]. Given the fact that aortic samples of AR patients revealed more severe inflammation, this may potentially lead to MMP activation and subsequent elastin fragmentation, which in turn causes replacement of elastic fibers with a fibro-collagenous extracellular matrix. These structural alterations lead to a weakening of aortic wall integrity, and loss of aortic elasticity, which may further progress into aortic dilation [2, 36, 37].

Although hemodynamic alterations may influence the progression of aortic dilation in AR patients, congenital factors seem to be more prevalent. This theory is supported by the fact that aortic dilation can also occur or progress following aortic valve surgery [18, 38]. Congenital factors

responsible for aortopathies may also account for the development of the associated AR [39]. This is because proximal aortic dilation is frequently associated with an aortic annulus dilation or a prolapse of the valve cusp. However, such considerations are still hypothetical and merit further prospective studies.

Despite the impact of an eccentric flow-jet on the aortic wall and increased WSS in AS patients, flow-generated effects were not obvious in the histological and gene expression comparison between the outer and the inner curvature. Interestingly, our AS patients who presented with an aortic diameter ≥40 mm were notably older as compared to those with normal-sized ascending aorta. At molecular level, the aging of extracellular matrix (ECM) is associated with molecular alterations in the long half-life proteins, such as elastin and collagen, and increased activity of oxidative stress. This excessive ECM remodeling has a critical impact on the vascular wall homeostasis [40]. This implies that the aging process is potentially involved in the pathogenesis of aneurysms in AS patients, as an older aorta becomes more susceptible to progressive dilation.

Younger age but no histological differences in bicuspid aortic regurgitation versus stenosis (comparison 2)

Due to the high number of BAV patients in our study population, we decided to compare both BAV patients with AS vs. AR. Numerous studies have documented that the malformed BAV impacts aortic hemodynamics predominantly by altering the direction of outflow jets, resulting in eccentric WSS distribution along the aortic vessel wall [41]. Comparison of pro-inflammatory as well as the medial degeneration gene markers did not reveal any significant differences between AR-BAV vs. AS- BAV subgroups. The possible explanation might be, that regardless of the type of valve dysfunction, all BAV patients experience increased WSS during their life-time that causes a persistent damage to the aortic wall over the years [42]. Even though both subgroups showed similar aortic wall alterations, it is extremely important to highlight that AR-BAV patients were significantly younger and had significantly larger aortic diameters. This finding indicates that aortic remodeling in AR-BAV patients occurs faster than in the AS-BAV patients. Similar finding were presented by Yongski and colleagues, who demonstrated that AR-BAV patients had a faster proximal aorta dilatation rate and a higher risk for adverse aortic events after an isolated AVR [18]. Based on this observations we were able to confirm that independently of the BAV morphology, regurgitation patients develop faster vascular lesions [26]. As we mentioned previously, we believe

that aortopathies in AR patients have a strong genetic predisposition to aortic wall weakness, which can be exacerbated by altered WSS.

Younger age but less medial degeneration in bicuspid aortic regurgitation versus tricuspid aortic regurgitation (comparison 3)

In our final analysis, we aimed to compare AR-BAV vs. AR-TAV patients with an AD ≥40 mm. Interestingly, we found that both subgroups had similar proximal aortic diameters. However, AR-BAV patients were a decade younger that AR-TAV patients. This age difference could be explained by the fact that aortic expansion rate is higher in BAV patients vs. TAV patients: 0.4 cm/y versus 0.2 cm/y [43]. Of note, children with a BAV have larger aortic diameters already at birth when compared to children with TAV [44]. Therefore, age correlates with aneurysm formation in BAV patients, and constitutes a major risk factor for cardiovascular events [43].

Regardless of our genetic expression and histological analysis, we were able to demonstrate that both AR subgroups had similar expression of inflammations markers in both aortic curvatures. On the contrary, the findings of our histological and medial degeneration gene analyses of the aortic tissue revealed a more pronounced medial degeneration (i.e., higher *COL1A1* gene expression, ELN fragmentation and CMD) in the AR-TAV patients vs. AR-BAV patients (Figure 5B, page 8). These findings are similar to those reported by Heng and coworkers. They observed that the extent of elastic fiber loss, smooth muscle cell loss, fibrosis, and atherosclerosis was more severe in TAV vs. BAV aortopathy patients with an AD between 4 and 5 cm [45]. Such differences in the extent of medial degeneration could be attributed to the age-related degeneration process. However, we cannot rule out the possibility that AR-TAV patients had an undiagnosed connective tissue disease at the time of the surgery.

Limitations

There are several limitations of our study, given the relatively small cohort size of tricuspid valve stenosis subgroup, the comparative analysis between AS-BAV vs. AS-TAV was not performed. Furthermore, we were not able to include relevant chemical parameters related to inflammation (i.e., LDH or HbA1c). Additionally, detailed hemodynamic data that could have impact on aortic wall changes such as LV ejection fraction, degree of the valve dysfunction and aortic valve gradients were also not available.

Summary

Our findings indicate that despite low WSS values in the proximal aorta, AR-patients demonstrated an increased inflammation and medial degeneration as compared to AS-patients. We also confirmed that, regardless of the valve morphology, the aortopathy in AR was characterized by younger patients' age and a more severe aortic dilation. Based on these findings, we should consider aortic regurgitation as a possible risk factor for proximal aortopathy and aortic complications. Therefore, we recommend that patients with AR and aortic diameter >40 mm should be closely monitored.

To validate our current findings, larger multicenter studies should be performed. We are currently planning to conduct prospective studies to evaluate the value of specific circulating biomarkers in the prediction of aortopathy progression. Furthermore, we are simultaneously collecting longitudinal data on MRI-based transvalvular flow patterns in patients with aortic valve dysfunction.

Zussammenfassung

Unsere Ergebnisse stellten heraus, dass AI-Patienten, trotz der niedrigen Wandschubspannung in der proximalen Aorta, eine erhöhte Inflammation und mediale Degeneration, im Vergleich zu AS-Patienten, aufwiesen. Wir konnten bestätigten, dass unabhängig von der Klappenmorphologie, die Aortopathie bei AI-Patienten, durch ein jüngeres Alter und eine stärkere Aortendilatation, gekennzeichnet war. Auf der Basis dieser Ergebnisse, sollten wir die Aortenklappeninsuffizienz, als möglichen Risikofaktor für proximale Aortopathie und Aorta Komplikationen, betrachten. Aufgrund dessen empfehlen wir, dass Patienten mit AI und Aortendurchmesser >40 mm engmaschiger überwacht werden sollten.

Um unsere bisherigen Ergebnisse zu bestätigen, sollten größere, multizentrische Studien durchgeführt werden. Wir planen derzeit die Durchführung prospektiver Studien, um den Wert spezifischer zirkulierender Biomarker, zur Vorhersage des Fortschreitens der Aortopathie, zu evaluieren. Darüber hinaus, sammeln wir gleichzeitig longitudinale Daten zu MRI-basierten, transvalvulären Flussmustern bei Patienten mit Aortenklappenerkrankungen.

Bibliography

1. Akinseye OA, Pathak A, Ibebuogu UN. Aortic Valve Regurgitation: A Comprehensive Review. *Curr Probl Cardiol.* 2018;43:315-334.

2. Anidjar S, Dobrin PB, Eichorst M, Graham GP, Chejfec G. Correlation of inflammatory infiltrate with the enlargement of experimental aortic aneurysms. *J Vasc Surg.* 1992;16:139-147.

3. Atkins SK, Sucosky P. Etiology of bicuspid aortic valve disease: Focus on hemodynamics. *World J Cardiol.* 2014;6:1227-1233.

4. Azadani AN, Chitsaz S, Mannion A, et al. Biomechanical properties of human ascending thoracic aortic aneurysms. *Ann Thorac Surg.* 2013;96:50-58.

5. Bjorck HM, Renner J, Maleki S, et al. Characterization of shear-sensitive genes in the normal rat aorta identifies Hand2 as a major flow-responsive transcription factor. *PLoS One.* 2012;7:e52227.

6. Borger MA, Fedak PWM, Stephens EH, et al. The American Association for Thoracic Surgery consensus guidelines on bicuspid aortic valve-related aortopathy: Executive summary. *J Thorac Cardiovasc Surg.* 2018;156:473-480.

7. Boudoulas KD, Wolfe B, Ravi Y, Lilly S, Nagaraja HN, Sai-Sudhakar CB. The aortic stenosis complex: aortic valve, atherosclerosis, aortopathy. *Journal of Cardiology.* 2015;65:377-382.

8. Boudoulas KD, Wolfe B, Ravi Y, Lilly S, Nagaraja HN, Sai-Sudhakar CB. The aortic stenosis complex: aortic valve, atherosclerosis, aortopathy. *J Cardiol.* 2015;65:377-382.

9. Chiu JJ, Chien S. Effects of disturbed flow on vascular endothelium: pathophysiological basis and clinical perspectives. *Physiol Rev.* 2011;91:327-387.

10. Cozijnsen L, Braam RL, Waalewijn RA, et al. What is new in dilatation of the ascending aorta? Review of current literature and practical advice for the cardiologist. *Circulation.* 2011;123:924-928.

11. Dewaswala N, Chait R. Aortic Regurgitation. *StatPearls*. Treasure Island (FL): StatPearls Publishing Copyright © 2020, StatPearls Publishing LLC.; 2020.

12. Dhawan SS, Avati Nanjundappa RP, Branch JR, et al. Shear stress and plaque development. *Expert Rev Cardiovasc Ther.* 2010;8:545-556.

13. Duca L, Blaise S, Romier B, et al. Matrix ageing and vascular impacts: focus on elastin fragmentation. *Cardiovasc Res.* 2016;110:298-308.

14. Elefteriades JA, Sang A, Kuzmik G, Hornick M. Guilt by association: paradigm for detecting a silent killer (thoracic aortic aneurysm). *Open Heart.* 2015;2:e000169.

15. Erbel R, Aboyans V, Boileau C, et al. 2014 ESC Guidelines on the diagnosis and treatment of aortic diseases: Document covering acute and chronic aortic diseases of the thoracic and abdominal aorta of the adult. The Task Force for the Diagnosis and Treatment of Aortic Diseases of the European Society of Cardiology (ESC). *Eur Heart J.* 2014;35:2873-2926.

16. Falk V, Baumgartner H, Bax JJ, et al. 2017 ESC/EACTS Guidelines for the management of valvular heart disease. *Eur J Cardiothorac Surg.* 2017;52:616-664.

17. Fedak PW, de Sa MP, Verma S, et al. Vascular matrix remodeling in patients with bicuspid aortic valve malformations: implications for aortic dilatation. *J Thorac Cardiovasc Surg.* 2003;126:797-806.

18. Folkersen L, Wagsater D, Paloschi V, et al. Unraveling divergent gene expression profiles in bicuspid and tricuspid aortic valve patients with thoracic aortic dilatation: the ASAP

study. *Mol Med.* 2011;17:1365-1373.
19. Girdauskas E, Rouman M, Disha K, et al. Functional Aortic Root Parameters and Expression of Aortopathy in Bicuspid Versus Tricuspid Aortic Valve Stenosis. *J Am Coll Cardiol.* 2016;67:1786-1796.
20. Gnus J, Witkiewicz W, Hauzer W, et al. Biomechanical definition of mechanical properties of the normal abdominal aortic walls and abdominal aortic aneurysm walls2011:15-21.
21. Goyal A, Keramati AR, Czarny MJ, Resar JR, Mani A. The Genetics of Aortopathies in Clinical Cardiology. *Clin Med Insights Cardiol.* 2017;11:1179546817709787.
22. Grewal N, Girdauskas E, DeRuiter M, et al. The role of hemodynamics in bicuspid aortopathy: a histopathologic study. *Cardiovasc Pathol.* 2019;41:29-37.
23. Halushka MK, Angelini A, Bartoloni G, et al. Consensus statement on surgical pathology of the aorta from the Society for Cardiovascular Pathology and the Association For European Cardiovascular Pathology: II. Noninflammatory degenerative diseases - nomenclature and diagnostic criteria. *Cardiovasc Pathol.* 2016;25:247-257.
24. Heng E, Stone JR, Kim JB, Lee H, MacGillivray TE, Sundt TM. Comparative Histology of Aortic Dilatation Associated With Bileaflet Versus Trileaflet Aortic Valves. *Ann Thorac Surg.* 2015;100:2095-2101; discussion 2101.
25. Hiratzka LF, Bakris GL, Beckman JA, et al. 2010 ACCF/AHA/AATS/ACR/ASA/SCA/SCAI/SIR/STS/SVM guidelines for the diagnosis and management of patients with Thoracic Aortic Disease: a report of the American College of Cardiology Foundation/American Heart Association Task Force on Practice Guidelines, American Association for Thoracic Surgery, American College of Radiology, American Stroke Association, Society of Cardiovascular Anesthesiologists, Society for Cardiovascular Angiography and Interventions, Society of Interventional Radiology, Society of Thoracic Surgeons, and Society for Vascular Medicine. *Circulation.* 2010;121:e266-369.
26. Kim HW, Stansfield BK. Genetic and Epigenetic Regulation of Aortic Aneurysms. *Biomed Res Int.* 2017;2017:7268521.
27. Lu MT, Thadani SR, Hope MD. Quantitative assessment of asymmetric aortic dilation with valve-related aortic disease. *Acad Radiol.* 2013;20:10-15.
28. Maiellaro K, Taylor WR. The role of the adventitia in vascular inflammation. *Cardiovasc Res.* 2007;75:640-648.
29. Maleki S, Bjorck HM, Folkersen L, et al. Identification of a novel flow-mediated gene expression signature in patients with bicuspid aortic valve. *J Mol Med (Berl).* 2013;91:129-139.
30. Martufi G, Forneris A, Appoo JJ, Di Martino ES. Is There a Role for Biomechanical Engineering in Helping to Elucidate the Risk Profile of the Thoracic Aorta? *Ann Thorac Surg.* 2016;101:390-398.
31. Mokashi SA, Svensson LG. Guidelines for the management of thoracic aortic disease in 2017. *Gen Thorac Cardiovasc Surg.* 2019;67:59-65.
32. Nayak L, Lin Z, Jain MK. "Go with the flow": how Kruppel-like factor 2 regulates the vasoprotective effects of shear stress. *Antioxid Redox Signal.* 2011;15:1449-1461.
33. Padang R, Bannon PG, Jeremy R, et al. The genetic and molecular basis of bicuspid aortic valve associated thoracic aortopathy: a link to phenotype heterogeneity. *Ann Cardiothorac Surg.* 2013;2:83-91.
34. Papaioannou TG, Stefanadis C. Vascular wall shear stress: basic principles and methods.

Hellenic J Cardiol. 2005;46:9-15.

35. Patel PA, Bavaria JE, Ghadimi K, et al. Aortic Regurgitation in Acute Type-A Aortic Dissection: A Clinical Classification for the Perioperative Echocardiographer in the Era of the Functional Aortic Annulus. *J Cardiothorac Vasc Anesth.* 2018;32:586-597.

36. Reimold SC, Maier SE, Aggarwal K, et al. Aortic flow velocity patterns in chronic aortic regurgitation: implications for Doppler echocardiography. *J Am Soc Echocardiogr.* 1996;9:675-683.

37. Robicsek F, Sanger PW, Taylor FH, Magistro R, Foti E. Pathogenesis and significance of post-stenotic dilatation in great vessels. *Ann Surg.* 1958;147:835-844.

38. Seitelberger R, Steindl J, Dinges C. Aortenklappeninsuffizienz. *Zeitschrift für Herz-,Thorax- und Gefäßchirurgie.* 2019;33:6-14.

39. Shan Y, Li J, Wang Y, et al. Aortic shear stress in patients with bicuspid aortic valve with stenosis and insufficiency. *J Thorac Cardiovasc Surg.* 2017;153:1263-1272 e1261.

40. Siu SC, Silversides CK. Bicuspid aortic valve disease. *J Am Coll Cardiol.* 2010;55:2789-2800.

41. Stone JR, Bruneval P, Angelini A, et al. Consensus statement on surgical pathology of the aorta from the Society for Cardiovascular Pathology and the Association for European Cardiovascular Pathology: I. Inflammatory diseases. *Cardiovasc Pathol.* 2015;24:267-278.

42. Tadros TM, Klein MD, Shapira OM. Ascending aortic dilatation associated with bicuspid aortic valve: pathophysiology, molecular biology, and clinical implications. *Circulation.* 2009;119:880-890.

43. Wagenseil JE. Bio-chemo-mechanics of thoracic aortic aneurysms. *Curr Opin Biomed Eng.* 2018;5:50-57.

44. Wang Y, Wu B, Li J, Dong L, Wang C, Shu X. Impact of Aortic Insufficiency on Ascending Aortic Dilatation and Adverse Aortic Events After Isolated Aortic Valve Replacement in Patients With a Bicuspid Aortic Valve. *Ann Thorac Surg.* 2016;101:1707-1714.

45. Youssefi P, Gomez A, He T, et al. Patient-specific computational fluid dynamics-assessment of aortic hemodynamics in a spectrum of aortic valve pathologies. *J Thorac Cardiovasc Surg.* 2017;153:8-20 e23.

3. Contribution(s) of each author

The table below presents the substantive contribution(s) of each author.

	Author Name	Conception and design	Analysis and interpretation	Writing the article	Critical revision of the article	Final approval of the article	Data collection	Provision of materials, patients, or resources	Statistical expertise	Obtaining funding	Literature search	Administrative, technical, or logistic support
1.	Tatiana Maria Sequeira Gross	✔	✔	✔	✔	✔	✔	✔			✔	
2.	Diana Lindner	✔	✔	✔	✔	✔					✔	
3.	Francisco M. Ojeda		✔		✔	✔			✔			✔
4.	Johannes T. Neumann				✔							✔
5.	Nimrat Grewal				✔			✔				✔
6.	Thomas Kuntze				✔		✔	✔		✔		
7.	Stefan Blankenberg				✔	✔		✔				
8.	Hermann Reichenspurner				✔	✔		✔		✔		
9.	Dirk Westermann	✔	✔	✔	✔	✔				✔	✔	
10.	Evaldas Girdauskas	✔	✔	✔	✔	✔	✔	✔		✔	✔	

4. Acknowlegments

I would like to extend my sincere thanks to Prof. Dr. med. Girdauskas, Prof. Dr. med. Westermann and PhD. Diana Lindner for the constant care and support throughout the study.

We also thank Mareile Schröder for her excellent technical assistance and PhD. Francisco Ojeda for the support with the statistical evaluation.

I especially thank the patients for allowing my study.

5. Curriculum Vitae

Lebenslauf wurde aus datenschutzrechtlichen Gründen entfernt.

6. Eidesstattliche Erklärung

Ich versichere ausdrücklich, dass ich die Arbeit selbständig und ohne fremde Hilfe verfasst habe, andere als die von mir angegebenen Quellen und Hilfsmittel nicht benutzt und die aus den benutzten Werken wörtlich oder inhaltlich entnommenen Stellen einzeln nach Ausgabe (Auflage und Jahr des Erscheinens), Band und Seite des benutzten Werkes kenntlich gemacht habe.

Ferner versichere ich, dass ich die Dissertation bisher nicht einem Fachvertreter an einer anderen Hochschule zur Überprüfung vorgelegt habe oder mich anderweitig um Zulassung zur Promotion beworben habe.

Ich erkläre mich einverstanden, dass meine Dissertation vom Dekanat der Medizinischen Fakultät mit einer gängigen Software zur Erkennung von Plagiaten überprüft werden kann.

Unterschrift: …….